Cell Reports

Resource

Global profiling of the proteomic changes associated with the post-testicular maturation of mouse spermatozoa

Graphical abstract

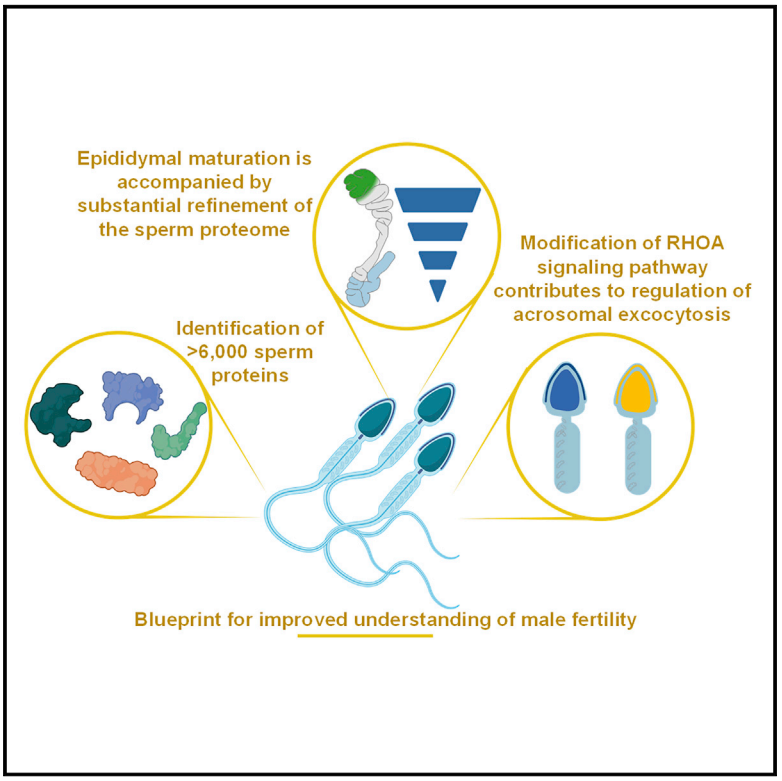

Authors

David A. Skerrett-Byrne, Amanda L. Anderson, Elizabeth G. Bromfield, ..., Matthew D. Dun, Sean J. Humphrey, Brett Nixon

Correspondence

david.skerrett-byrne@newcastle.edu.au (D.A.S.-B.), brett.nixon@newcastle.edu.au (B.N.)

In brief

Skerrett-Byrne et al. have characterized the epididymal sperm proteome undergoing functional maturation. Contrary to the long-held belief that epididymal maturation is primarily driven by the uptake/modification of additional proteins, this work demonstrates that spermatozoa shed over half their protein composition during this process.

Highlights

- Identification of >6,000 proteins provides insight into sperm cell proteome
- Sperm cell proteome is dramatically remodeled during post-testicular maturation
- Major changes are associated with the loss, as opposed to gain, of sperm proteins
- Activated RHOA-mediated signaling pathways contribute to functional maturity of sperm

Skerrett-Byrne et al., 2022, Cell Reports *41*, 111655
November 15, 2022
https://doi.org/10.1016/j.celrep.2022.111655

CellPress

Cell Reports

CellPress
OPEN ACCESS

Resource

Global profiling of the proteomic changes associated with the post-testicular maturation of mouse spermatozoa

David A. Skerrett-Byrne,[1,2,*] Amanda L. Anderson,[1,2] Elizabeth G. Bromfield,[1,2,3] Ilana R. Bernstein,[1,2] Jess E. Mulhall,[1,2] John E. Schjenken,[1,2] Matthew D. Dun,[4] Sean J. Humphrey,[5,6] and Brett Nixon[1,2,7,*]

[1]Priority Research Centre for Reproductive Science, School of Environmental and Life Sciences, Discipline of Biological Sciences, The University of Newcastle, University Drive, Callaghan, NSW 2308, Australia

[2]Hunter Medical Research Institute, Infertility and Reproduction Research Program, New Lambton Heights, NSW 2305, Australia

[3]Department of Biomolecular Health Sciences, Faculty of Veterinary Medicine, Utrecht University, Utrecht, the Netherlands

[4]Cancer Signalling Research Group, School of Biomedical Sciences and Pharmacy, College of Health, Medicine and Wellbeing, Hunter Medical Research Institute, University of Newcastle, Callaghan, NSW, Australia

[5]School of Life and Environmental Sciences, The University of Sydney, Sydney, NSW, Australia

[6]The Charles Perkins Centre, The University of Sydney, John Hopkins Drive, Camperdown, NSW 2006, Australia

[7]Lead contact

*Correspondence: david.skerrett-byrne@newcastle.edu.au (D.A.S.-B.), brett.nixon@newcastle.edu.au (B.N.)

https://doi.org/10.1016/j.celrep.2022.111655

SUMMARY

Spermatozoa acquire fertilization potential during passage through a highly specialized region of the extratesticular ductal system known as the epididymis. In the absence of *de novo* gene transcription or protein translation, this functional transformation is extrinsically driven via the exchange of varied macromolecular cargo between spermatozoa and the surrounding luminal plasma. Key among these changes is a substantive remodeling of the sperm proteomic architecture, the scale of which has yet to be fully resolved. Here, we have exploited quantitative mass spectrometry-based proteomics to define the extent of changes associated with the maturation of mouse spermatozoa; reporting the identity of >6,000 proteins, encompassing the selective loss and gain of several hundred proteins. Further, we demonstrate epididymal-driven activation of RHOA-mediated signaling pathways is an important component of sperm maturation. These data contribute molecular insights into the complexity of proteomic changes associated with epididymal sperm maturation.

INTRODUCTION

Prior to engaging in the cascade of cellular interactions that underpin fertilization, mammalian spermatozoa must first complete an arduous journey of functional maturation (Reid et al., 2011). This dynamic transformation of the spermatozoon is initiated within the seminiferous tubules of the testes as a subset of spermatogonial stem cells commit to differentiation. This complex process encompasses sequential mitotic and meiotic divisions followed by substantial remodeling of the cytoplasmic and nuclear architecture, eventually giving rise to arguably one of the most highly differentiated cells in the body (Hermo et al., 2010a). This specialization is reflected in the sperm chromatin structure, which is condensed to a near crystalline state owing to the replacement of histones by protamines; a process that eliminates the potential to actuate conventional pathways of gene transcription and protein translation (Hermo et al., 2010b). However, notwithstanding the substantial morphological specialization attained, sperm cells released from the testes lack the capacity for forward progressive motility, nor can they trigger productive interactions with the ovum (Zhou et al., 2018). Rather, the ability to fulfill these fundamental roles is progressively acquired during the protracted transport of spermatozoa through the epididymis. As sperm complete their migration of this highly differentiated region of the male excurrent duct system (Nixon et al., 2020), they undergo substantive remodeling of their proteomic (Aitken et al., 2007), lipid, and epigenetic architecture (Nixon et al., 2019a). This remodeling is driven by exposure to extrinsic factors that sperm encounter within the epididymal lumen (Bedford, 2015), which are predominantly secreted by the epithelium lining the proximal epididymal segments (Zhou et al., 2018). Consequently, mature spermatozoa carry discrete molecular signatures that readily discriminate them from their immature counterparts (Caballero et al., 2013). Despite this knowledge, the extent of the proteomic changes that maturing spermatozoa experience remains uncertain as does their contribution to specific aspects of sperm function. Pursuit of this knowledge gap will shed light on the level of the evolutionary complexity invested into epididymal maturation and provide a greater understanding of the key proteins that are essential for fertilization.

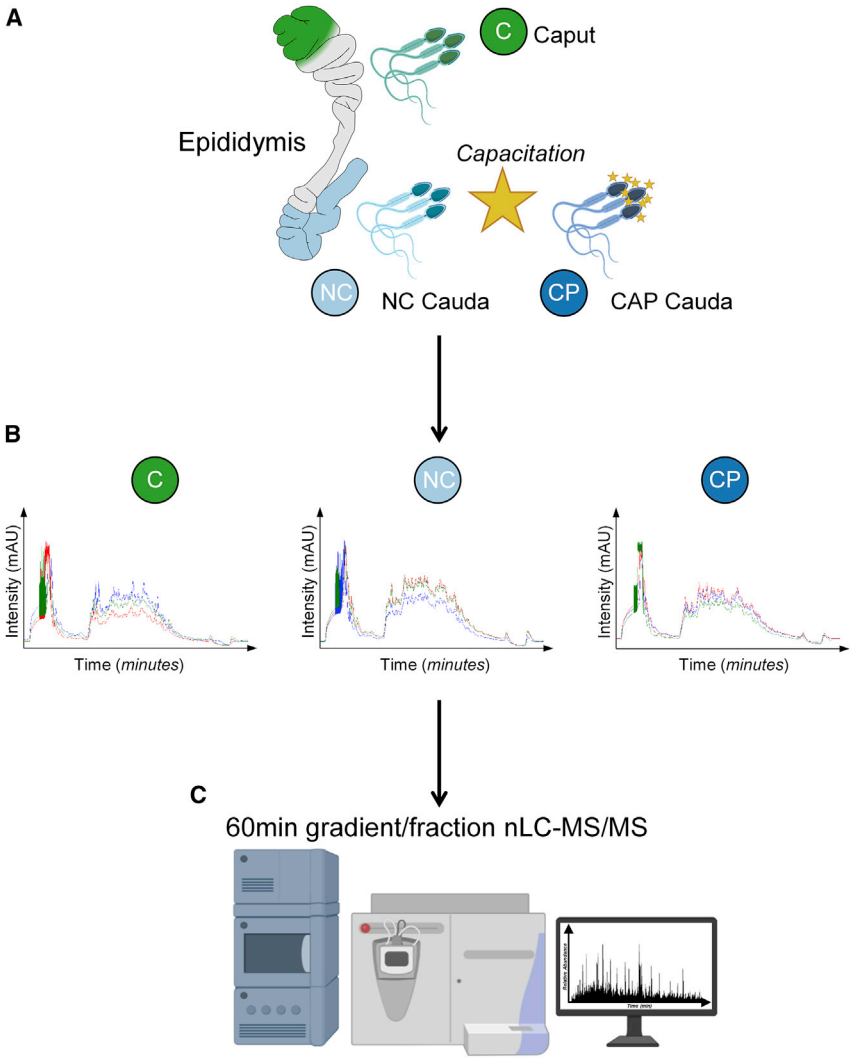

Figure 1. Experimental workflow for proteomic assessment of maturing epididymal mouse spermatozoa

(A) Mouse sperm cells were collected from the caput (proximal region, green) and cauda (distal region, light blue), and a portion of caudal spermatozoa were induced to undergo capacitation *in vitro* (dark blue).

(B) Following protein extraction and generation of tryptic peptides, each sample was deconvoluted in 12 sub-populations using offline high pH fraction.

(C) Each fraction was subjected to a 60-min gradient on an Orbitrap Exploris 480 mass spectrometer. Aspects of this figure were created with BioRender.com.

In seeking to address the challenges of these long-standing questions, attention has increasingly turned to the application of novel technological innovations in high-resolution mass spectrometry (MS) to map the sperm proteome. One such tool is label-free quantitative MS, a technique enabling both relative and absolute quantification of cellular proteins. In the absence of chemical modifications, this technology relies on a workflow in which individual samples are analyzed separately prior to protein quantitation via either ion profiling or spectral counting. Such approaches have been used to construct proteomic inventories of sperm harboring functional lesions associated with idiopathic infertility, yielding key molecular insight into the changes associated with this pathology (Redgrove et al., 2012), including the identification of sperm proteins that provide a robust discriminative index of the success of cumulus-oocyte interactions and fertilizing potential (Cayli et al., 2003; Ergur et al., 2002; Nixon et al., 2015a, 2017). Such fundamental information holds considerable promise for identifying key biomarkers of male fertility in addition to elements of the sperm proteome that might be targeted for fertility regulation both in the context of contraceptive development and therapeutic intervention (Dun et al., 2010). Nevertheless, the potential of comparative proteomic strategies has yet to be fully realized in terms of characterizing the inventory of proteins that differentiate immature spermatozoa from that of their mature counterparts. Accordingly, here we apply a cutting-edge, label-free quantitative MS workflow to identify changes in the mouse sperm proteome associated with their passage to maturity within the epididymis.

RESULTS

Characterization of the maturing mouse sperm proteome

To characterize the proteomic alterations to sperm during epididymal maturation, we isolated highly enriched populations of functionally immature and mature spermatozoa from the caput (proximal) and cauda (distal) segments of the mouse epididymis, respectively (Figure S1A). To differentiate epididymal-driven changes to the sperm proteome from those elicited in response to capacitation (i.e., a sequence of biochemical and biophysical changes that prime spermatozoa for fertilization as they ascend the female reproductive tract), we induced a subset of the caudal sperm population to undergo capacitation *in vitro* prior to cell lysis (Figure 1A). Following protein extraction and digestion, peptides were subjected to offline high pH fractionation (Figure 1B) and analyzed by high-resolution nLC-MS/MS (Figure 1C). Assessment of the correlation between biological replicates demonstrated high reproducibility, with an average Pearson's correlation of 0.97 (Figure 2A). Proteomic profiling confirmed an unprecedented depth of coverage in our sperm proteomic inventories (false discovery rate [FDR] $\leq$ 0.01) with 6,045, 2,924, and 2,814 proteins identified in caput, non-capacitated (NC) cauda and capacitated (CAP) cauda samples, respectively (Figure 2B and Table S1). Among these inventories, an average number of 10.3 (caput), 10.3 (NC cauda), and

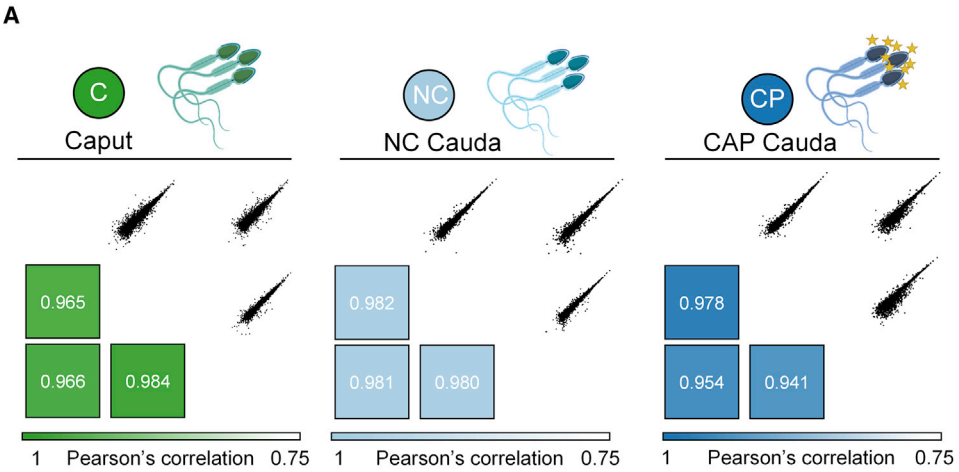

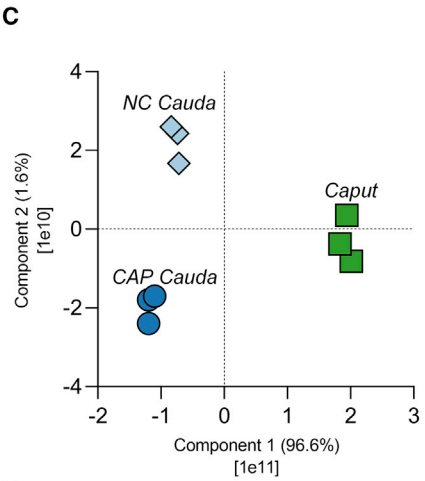

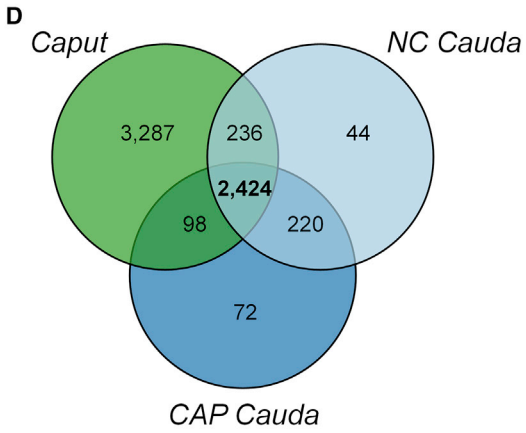

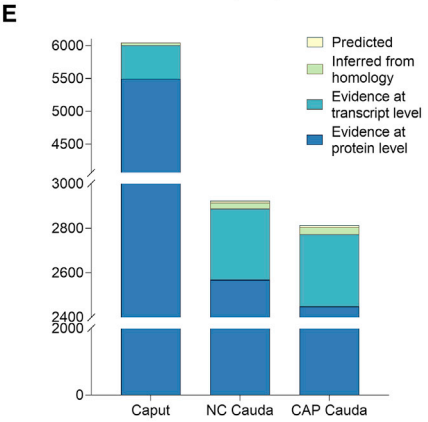

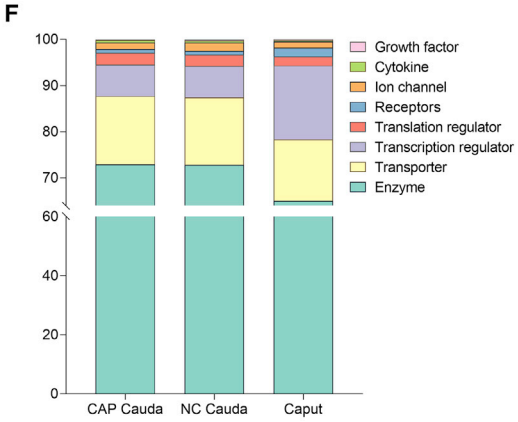

(legend on next page)

10.6 (CAP cauda) unique peptides were identified per protein, encompassing an average protein coverage of 29.0%, 32.3%, and 33.5%, respectively (Figure 2B and Table S1). In support of the high reproducibility indicated by Pearson correlations (Figure 2A), principal component analysis (PCA) also revealed a high level of concordance among the biological replicates comprising each sample group (Figure 2C). Notably, PCA also confirmed that each sub-population of spermatozoa was clearly differentiated on the basis of their core proteome. In particular, caput epididymal sperm replicates were found to reside directly opposed to those of the cauda epididymal spermatozoa, with component one accounting for 96.6% of this observed variance.

Direct comparison of the three sperm populations demonstrated a shared proteomic signature of 2,424 proteins (Figure 2D). Most strikingly, this analysis revealed over 3,000 proteins that were identified exclusively in the immature caput epididymal sperm and were not detected in their mature cauda epididymal sperm counterparts. This substantial protein loss was accompanied by the acquisition of 336 proteins uniquely identified in cauda epididymal spermatozoa. Assessment of the curated evidence (UniProt) supporting the existence of each identified protein across all three sperm populations revealed 661 proteins with no previous evidence at the protein level (Figure 2E and Table S1), comprising 603 proteins with only transcript evidence (9.4%), 49 inferred from homology (0.8%), and 9 predicted (0.1%). Notwithstanding this limited annotation and the attendant prospect that spermatozoa and/or epididymal tissue may harbor cell/tissue-specific proteins, compositional analysis of each sperm sample revealed their proteomes broadly consisted of enzymes (61.8%), kinases (6.7%), phosphatases (4.3%), and ion channels (1.8%) (Figure 2F and Table S1). No overt changes in the categorization of sperm proteins accompanied their epididymal maturation, except for a proportional decrease in transcription regulators, which represented 16.0% of all proteins detected in immature caput epididymal spermatozoa and only 6.8% in mature cauda epididymal spermatozoa (Figure 2F and Table S1). Additional *in silico* analyses using UniProt and EMBL-EBI GO annotations mapped 50.7% of identified proteins (3,234) to a specific sperm cell domain (i.e., acrosome, perinuclear theca, nucleus, mitochondria, mid-piece, annulus, axoneme, and flagellum), with the majority of these proteins (2,436) associated with the nucleus (Figure S1B).

Remodeling of the sperm proteome during epididymal maturation

Immature sperm cells isolated from the caput epididymis harbored the most complex proteome of the three samples analyzed, comprising 6,045 proteins, including 1,284 (93.9%) of all proteins previously identified in independent studies of mouse caput epididymal sperm cells (Figure 3A) (Skerget et al., 2015), thereby extending the proteomic annotation of this sperm population by an additional 4,761 proteins (Figure 3A). However, we identified a dramatic reduction in the number of proteins comprising the mature sperm proteome, with as many as 3,385 proteins apparently being lost from spermatozoa during their epididymal transit. Notably, while this proportional loss of 56% of the sperm proteome may appear at odds with accepted paradigms of sperm maturation, it nevertheless draws striking parallels to the 42% loss of the sperm proteome reported in the only other large-scale proteomic investigation of mouse epididymal spermatozoa by Skerget et al. (Skerget et al., 2015) (Figures 3A and S2). Notwithstanding a substantial loss of proteins coincident with epididymal transit, cauda epididymal sperm cells retained a core proteome of 2,660 proteins in common with their caput epididymal sperm counterparts (Figure 3B). This core proteome was supplemented by the addition of 264 proteins uniquely detected in NC cauda epididymal spermatozoa, a proportional gain of 9% of the total proteome (Figure 3B). The proteome (2,924 proteins) of mature cauda epididymal sperm included 87.9% of the proteins (i.e., 1,062 proteins) identified by Skerget and colleagues in their proteomic study of mouse spermatozoa (Skerget et al., 2015), as well as an additional 1,999 proteins that were not previously characterized (Figure 3B).

Accordingly, to confirm the differential abundance of proteins identified in our label-free proteomic data, we employed immunoblotting as an orthogonal technique to assess the relative abundance of a subset of these proteins, as well as assessment of localization by immunocytochemistry. Chief among the down-regulated proteins were protein disulfide-isomerase A6 (PDIA6), RNA-binding protein Musashi homolog 2 (MSI2), and 14-3-3 protein sigma (14-3-3). In accordance with our proteomic analyses, each of these proteins were detected in the immature caput epididymal sperm population yet were significantly underrepresented in their mature cauda epididymal sperm counterparts (Figure 3C; PDIA6, fold change [FC] = −10.2; MSI2, FC = −2.8; and 14-3-3, FC = −10.4), findings that were in agreement with immunocytochemical labeling of the target proteins (Figure S3). To validate protein acquisition/increases, we also assessed a subset of candidate proteins by immunoblotting. Calcium-binding tyrosine phosphorylation-regulated protein (CABYR) and adenylyl cyclase 10 (ADCY10) demonstrated a marked increase in abundance in cauda epididymal sperm compared with the caput epididymal sperm population (Figure 3D; CABYR,

Figure 2. Proteomic characterization of functionally immature and mature mouse spermatozoa

(A) Pearson correlation plots of biological replicates for caput (immature, green), non-capacitated cauda (mature, light blue), and capacitated cauda (dark blue) epididymal sperm populations.

(B) The total number of proteins identified within each population's proteomic signature, caput (6,045), NC cauda (2,924), and CAP cauda (2,814), along with the average number of unique peptides/protein and average protein coverage (%).

(C) Principal component analysis (PCA) of the proteome of each sperm cell population with their respective biological replicates; caput (green squares), NC cauda (light blue diamonds), and CAP cauda (dark blue circles).

(D) Venn diagrams depict the shared and unique number of proteins with all three populations.

(E) UniProt annotation of level of evidence for protein existence.

(F) Classification of protein types by Ingenuity Pathway Analysis respresented as a proportion of all proteins identified.

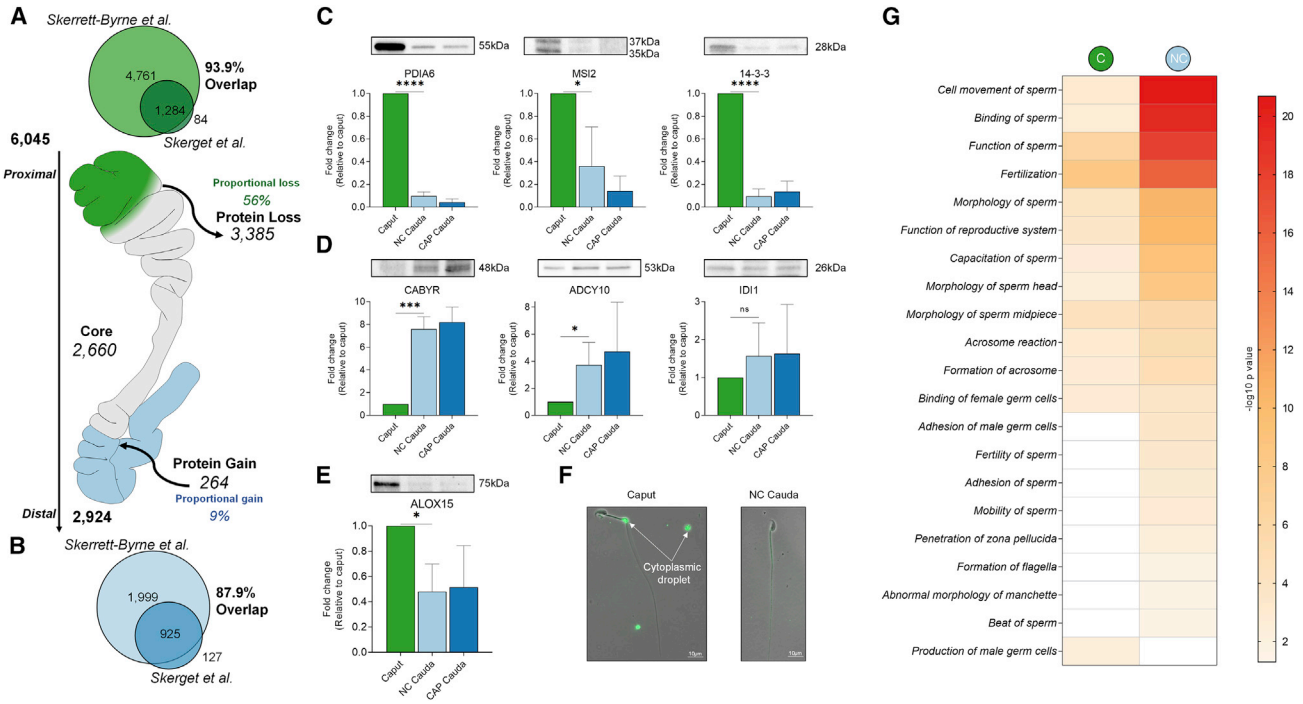

Figure 3. Epididymal transit is accompanied by substantial remodeling of the maturing sperm proteome

(A) The total number of proteins identified in immature caput (proximal) epididymal sperm, compared with cauda (distal) epididymal sperm, identifying proteins lost (3,385) during epididymal maturation. A comparison to the previous characterization of the caput epididymal sperm proteome reported by Skerget et al. (Skerget et al., 2015) is included.

(B) The complete protein signature of cauda epididymal sperm, identifying 264 unique proteins added during maturation, compared with previous proteome characterization.

(C) Immunoblotting validation of lost/downregulated proteins, protein disulfide-isomerase A6 (PDIA6), RNA-binding protein Musashi homolog 2 (MSI2), and 14-3-3 protein sigma.

(D) Epididymal acquired/upregulated proteins calcium-binding tyrosine phosphorylation-regulated protein (CABYR) and adenylyl cyclase 10 (ADCY10) assessed by immunoblotting, as well as confirmation of retained protein isopentenyl-diphosphate delta-isomerase 1 (IDI1).

(E and F) Immunoblotting confirmation of arachidonate 15-lipoxygenase (ALOX15) and (F) immunofluorescence of caput and cauda epididymal sperm (white arrows indicating the cytoplasmic droplet); scale bar of 10 μm included. All immunoblotting experiments were repeated with at least three biological replicates, and densitometric data normalization was performed against the loading control protein GAPDH. Data were analyzed by unpaired t test; * p value $\leq$ 0.05; ** p value $\leq$ 0.01; *** p value $\leq$ 0.001.

(G) Molecular and biological processes associated with the proteome of caput and cauda epididymal sperm were assessed by Ingenuity Pathway Analysis; only significant (p value $\leq$ 0.05) processes are presented.

FC = 7.6; ADCY10, FC = 3.7). This was supported by the immunolabeling of CABYR predominately within the sperm flagellum (Figure S3), whereas ADCY10 was detected in the principle piece and peri-acrosomal region of the sperm head (Figure S3). Adding to this validation strategy, immunoblotting and immunocytochemistry confirmed the abundance of sperm proteins such as isopentenyl-diphosphate delta-isomerase 1 (IDI1) remained unchanged during epididymal maturation (Figures 3D and S3). Moreover, immunoblotting of immature and mature sperm lysates confirmed that a significant reduction in the abundance of arachidonate 15-lipoxygenase (ALOX15) occurred during epididymal maturation (Figure 3E; ALOX15, FC = −2.1). Investigation of ALOX15 localization with immunocytochemistry revealed residency predominantly in the cytoplasmic droplet in caput epididymal sperm cells (Figure 3F), consistent with a previously reported role in cytoplasmic droplet shedding during epididymal maturation (Moore et al., 2010).

Ingenuity Pathway Analysis (IPA) of the core sperm proteomes identified 24 key biological processes related to male reproduction and sperm function. Notably, despite the caput epididymal sperm cells harboring over 3,000 more proteins than their cauda epididymal counterparts, the latter featured significant enrichment scores for each of these specific biological processes (Figure 3G), a finding that resonates with the importance of the epididymis in promoting the functional maturation of spermatozoa. Specifically, the most significant biological processes that mapped to the mature cauda epididymal sperm proteome included "cell movement," "binding of female germ cells," and "function of sperm." Furthermore, critical fertilization processes such as "capacitation of sperm" and "formation and reaction of the acrosome" were also more highly enriched in the proteome of the mature caudal sperm population. Moreover, "penetration of the zona pellucida" was a biological process uniquely enriched in caudal epididymal spermatozoa (Figure 3G). By

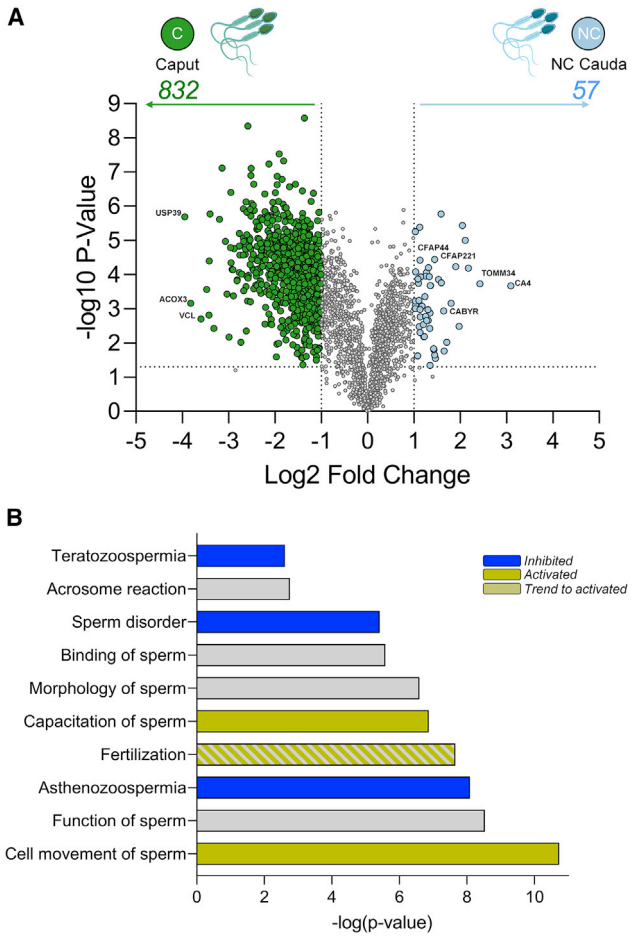

Figure 4. Quantitative analysis identifies proteins associated with sperm maturation

(A) Volcano plot depicting the core sperm proteome (2,660) and the differential abundance of 889 proteins associated with epididymal maturation; log2 fold change (x axis) and –log p value (y axis) with thresholds of ±2 fold change and p value $\leq$ 0.05.

(B) Top ten sperm molecular and biological processes identified by Ingenuity Pathway Analysis ($p \leq 0.05$), including predicted activation (Z score ≥ 2, gold) or inhibition (Z score ≤ -2, blue) of functions associated with epididymal maturation. Gray denotes no significant Z score, and gold with diagonal gray stripes denotes processes with Z score of 1.98.

contrast, the only biological process enrichment unique to caput spermatozoa was the "production of male germ cells," which is in accordance with this epididymal segment being populated by immature sperm cells harboring residual cytoplasm in the form of a cytoplasmic droplet, a legacy of their spermatogenic development within the testes.

Epididymal transit is accompanied by substantive remodeling of the sperm proteomic architecture

Concentrating on the core proteome retained by spermatozoa during epididymal maturation, we compared the quantitative differences in protein abundance between the immature caput and mature cauda epididymal sperm cells. This analysis revealed 889 sperm proteins whose abundance was significantly altered as the cells transited the epididymis (FC ± 2, p value $\leq$ 0.05) (Figure 4A and Table S1). Consistent with the substantial protein losses documented above (Figure 3), the overwhelming majority of these proteins (i.e., 832/889 proteins; 94%) were underrepresented in cauda epididymal spermatozoa. The largest changes observed were associated with U4/U6.U5 tri-snRNP-associated protein 2 (USP39; FC = −15.4), peroxisomal acyl-coenzyme A oxidase 3 (ACOX3; FC = −14.1), and vinculin (VCL; FC = −12.1). Other notable downregulated proteins included motile sperm domain-containing protein 2 (MOSPD2; FC = −5.3), prosaposin (PSAP; FC = −5.1), and PDIA6 (FC = −4.6). By contrast, a comparatively modest subset of 57 proteins were overrepresented in cauda epididymal sperm compared with their caput epididymal counterparts. Chief among these were several proteins that have previously been implicated in the regulation of sperm motility including carbonic anhydrase 4 (CA4; FC = 8.5), cyclic nucleotide-binding domain-containing protein 2 (CNBD2; FC = 1.9), and cilia- and flagella-associated proteins (CFAP) 44 (FC = 2.2), CFAP100 (FC = 2.0), and CFAP221 (FC = 2.7). Moreover, we observed marked increases in calcium-binding tyrosine phosphorylation-regulated protein CABYR (FC = 3.1). By way of validating these data, we assessed the abundance of PDIA6 and CABYR by immunoblotting of sperm cell lysates prepared using extraction protocols of differing stringency. While the extraction protocol can indeed influence the efficacy of sperm protein recovery (Figure S4A), nevertheless PDIA6 was consistently observed in lower abundance in cauda versus caput epididymal sperm (Figure S4B), and the expected reciprocal relationship was detected for CABYR (Figure S4C), irrespective of the extraction protocol used.

In seeking to understand the biological processes associated with the protein compositional changes that accompany sperm maturation, we further interrogated the subset of proteins that were either significantly altered (down- and upregulated) and newly acquired during epididymal transit. Focusing once more on the reproductive and sperm-related functions (Figure 4B), we observed abundance changes in 79 proteins that led to the predicted activation of "cell movement of sperm" (Z score = 2.52) and "capacitation of sperm" (Z score = 2.83), as well as "fertilization" (Z score = 1.98). Moreover, this analysis revealed an inhibition of the known sperm disorders, "asthenozoospermia" (Z score = −2.65) and "teratozoospermia" (Z score = −2.01). To further complement these analyses, the curated list of protein changes (including complete gains and losses) was compared with entries in the Mouse Genome Informatics and the International Mouse Phenotyping Consortium databases to identify those proteins associated with male fertility phenotypes and/or impaired sperm function. This comparison identified 241 proteins that have previously been associated with 36 relevant phenotypes, including potential impairment to critical fertilization functions such as capacitation and acrosome reaction (Tables 1 and S2).

Sperm capacitation leads to subtle proteomic changes

Considering the relatively conserved proteomic composition of NC and CAP cauda epididymal sperm populations, our data identifies a subset of protein changes that could influence the capacitation cascade. This includes 19 proteins whose

abundance was increased, and a further 10 proteins that decreased in populations of CAP spermatozoa compared with that of their NC counterparts (Figure S5A and Table 2). We further interrogated this comparison using IPA, revealing key reproductive processes were significantly enriched, including "function of sperm," "cell movement of sperm," and "fertilization" (Figure S5B). Among these changes, the dominant upregulated protein was pyruvate kinase PKM (PKM; FC = 4.7), with additional upregulated proteins including ubiquitin-conjugating enzyme E2 H (UBE2H; FC = 3.7), putative ATP-dependent RNA helicase Pl10 (D1PAS1; FC = 2.59), and ubiquitin-conjugating enzyme E2 D3 (UBE2D3; FC = 2.15). Assessment of the latter three proteins by immunoblotting confirmed their putative increased abundance in sperm lysates following capacitation (Figure S5C; UBE2H, FC = 1.5; D1PAS1, FC = 1.4; UBE2D3, FC = 1.7). Alternatively, proteins that were underrepresented in the CAP sperm population included the splicing factor 3B subunit 1 (SF3B1; FC = −6.8), sodium/hydrogen exchanger 1 (SLC9A1; FC = −6.5), and protamine-2 (PRM2; FC = −5.5).

Epididymal sperm maturation contributes to the priming of RHOA-mediated signaling pathways associated with acrosomal exocytosis

In seeking to reconcile the pronounced functional changes accompanying epididymal sperm maturation with the documented changes in their proteome, we elected to focus on RHOA, a protein that was identified as being significantly more abundant in the proteome of mature cauda epididymal sperm compared with that of caput epididymal sperm (FC = 2.0). Interestingly, our MS data identified Rho GDP-dissociation inhibitor 1 (GDI-1), along with numerous additional RHOA interacting proteins involved in the RHOGDI signaling pathway (IPA; p value = 0.012) that are capable of repressing its activity, as being either significantly downregulated or completely lost from the proteome of cauda epididymal spermatozoa (Table S3). As a case in point, Rho GTPase-activating protein 18, which suppresses F-actin polymerization by inhibiting RHOA (Maeda et al., 2011), was exclusively detected in caput epididymal spermatozoa. Based on these data, we infer that immature caput epididymal sperm may harbor minimal and/or inactive RHOA, whereas cauda epididymal sperm are endowed with an elevated quantity, and possibly activity, of RHOA. To begin to explore if there is a functional consequence of this change, we subjected caput and cauda spermatozoa to selective pharmacological inhibition of RHOA using CT04, a treatment that compromises actin polymerization events such as those preceding induction of an acrosome reaction. Initial cytotoxicity testing, during which mouse spermatozoa were incubated with CT04 (0.5, 1.0, and 2.0 μg/mL) over a time course of up to 2 h (i.e., 0, 60, and 120 min), demonstrated this drug had no significant impact on sperm viability (Figure S6A). Similarly, using a concentration of 1.0 μg/mL (based on previous studies of guinea pig spermatozoa (Reyes-Miguel et al., 2020), we demonstrated that RHOA inhibition had no overt biological effect on the percentage of motile mouse spermatozoa (Figure 5A), nor those capable of undergoing capacitation (Figure 5B). By contrast, RHOA inhibition led to a significant reduction in the ability of CAP cauda epididymal spermatozoa to engage in acrosomal exocytosis (Figure 5C). In this context, CT04 significantly inhibited the rates of spontaneous acrosome reaction as well as those induced in the presence of the calcium ionophore A23187 (Figure 5C). Collectively, these data indicate that the absence of key intermediary protein signaling machinery, such as RHOA, may at least in part account for the inability to induce functional responses in immature caput epididymal spermatozoa.

DISCUSSION

A striking feature of the functional maturation that spermatozoa undergo after leaving the testes is that this developmental process occurs in the complete absence of endogenous gene transcription or *de novo* protein translation (Bedford, 2015; Nixon et al., 2019a, 2019b; Zhou et al., 2018). Thus, sperm procure their functional maturity as a consequence of modifications to their intrinsic proteome coincident with their ascension of the male (epididymal maturation) and female reproductive tracts (capacitation) (Baker et al., 2012). Improvements in our mechanistic understanding of these events is therefore predicated on a detailed assessment of the sperm proteomic architecture. Accordingly, herein we have utilized advancements in label-free quantitative MS to thoroughly map the protein composition of immature (caput; proximal epididymal segment) and mature spermatozoa (caudal; distal epididymal segment), delivering molecular insights into the core proteomic elements that constitute a fertilization-competent sperm cell. Indeed, our study reports the identification of over 6,000 sperm proteins, a depth of coverage that not only exceeds that of previous studies of mouse epididymal sperm (>4 fold increase in proteome coverage (Skerget et al., 2015) but also approaches the estimated 7,500 proteins that constitute the complete proteome of a human spermatozoon (Amaral et al., 2013). Moreover, we provide proteomic evidence for the identification of 661 proteins that are annotated within the mouse genome, but without previous confirmation at the protein level, thus raising the prospect that spermatozoa may harbor cell specific proteins.

Our data reveal that epididymal maturation is accompanied by large-scale remodeling of the sperm proteome, in agreement with previous work by Skerget et al. (Skerget et al., 2015), whereby 56% of the proteins identified in immature spermatozoa are apparently lost during their functional maturation, while only a relatively modest 9% of proteins are newly acquired. Exploiting the quantitative nature of our analysis, we identified that these changes were accompanied by a proportional loss and increase in the abundance of an additional 889 proteins. Notable among those proteins gained by maturing spermatozoa were several examples of candidates implicated in the regulation of sperm motility (ADCY10, CFAP proteins 44 and 221) (Esposito et al., 2004; Lee et al., 2008; McKenzie and Lee, 2020; Schmid et al., 2007; Tang et al., 2017), capacitation (CABYR) (Naaby-Hansen et al., 2002), and binding of the zona pellucida (DEFB22) (Tollner et al., 2004; Yudin et al., 2008). Furthermore, counterintuitive to the notion of gaining proteins to gain function, our data indicates that the sperm molecular landscape is refined to a substantially smaller proteome coinciding with the enrichment of key cellular processes, including "cell movement of sperm" and "capacitation of sperm," as well as "penetration of zona pellucida." These

Table 1. Associated reproductive phenotypes

Phenotype description	Number of associated proteins			
	Lost	Gained	Downregulated	Upregulated
Impaired functions/processes				
Acrosome reaction	2	1	3	
Capacitation	1	3		7
Fertility/infertility	181	28	59	10
Meiosis	26	5	9	
Mitochondrial function	9		4	
Motility	5	4	2	7
Sperm number	2		1	
Spermatogenesis	56	4	8	
Spermiogenesis	11	3	2	
Sperm disorders				
Oligozoospermia	56	6	13	2
Azoospermia	38		13	
Asthenozoospermia	26	9	2	2
Teratozoospermia	24	5	8	3
Globozoospermia	9	3		
Necrospermia	5			

findings reinforce the importance of epididymal maturation in shaping the sperm proteome to permit successful navigation of the female reproductive tract and ultimately fertilization. Conversely, the substantial loss and underrepresentation of proteins in cauda epididymal sperm yielded putative inhibition of sperm disorders such as "asthenozoospermia" and "teratozoospermia," adding further credence to the importance of epididymal sperm maturation to form a fertilization-competent cell. Indeed, many of the proteins that were substantially reduced in abundance in cauda epididymal sperm mapped to fertility phenotypes, indicating their importance prior to post-testicular sperm maturation. By way of example, ablation of the RNA demethylase ALKBH5 has previously been linked to significantly reduced sperm count (Zheng et al., 2013).

In terms of accounting for the mechanisms underpinning the substantial loss of sperm proteins, it is conceivable that these reflect adventitiously bound proteins that are present in very large abundance in, for example, the proximal segments of the extratesticular duct system (i.e., rete testis or efferent ducts) and that remain transiently adherent to the surface of caput epididymal sperm before being released or proteolytically cleaved during the cell's descent through the epididymis. Alternatively, such proteins may be indiscriminately shed along with the cytoplasmic droplet, small focal distensions of residual cytoplasm that are formed in the neck region of spermatozoa immediately prior to their release from the seminiferous epithelium of the testis (Au et al., 2015; Hermo et al., 2019). Thereafter, cytoplasmic droplets remain transiently adherent to the sperm surface while gradually migrating along the length of the flagellum and eventually being shed via mechanical shearing or enzymatic activities (Moore et al., 2010). It follows that the isolation protocols employed herein generated sperm populations in which approximately 40% of the cauda epididymal sperm cells had shed their cytoplasmic droplet (Hutcheon et al., 2017). Accordingly, our characterization of ALOX15, which is known to be a major contributor to the initiation of cytoplasmic droplet shedding (Moore et al., 2010), revealed notable localization within the cytoplasmic droplet in caput epididymal spermatozoa followed by a significant underrepresentation of the enzyme in their cauda epididymal counterparts. Despite cytoplasmic droplets being evolutionarily conserved in the spermatozoa of diverse vertebrate species (Yuan et al., 2013), the physiological roles of this vestigial organelle remain elusive (Hermo et al., 2019). In early, substrate-based biochemical analyses, cytoplasmic droplets were shown to possess lysosomal and glycolytic enzyme activities (Dott and Dingle, 1968; Garbers et al., 1970; Harrison and White, 1972; Roberts et al., 1976). This resonates with recent proteomic studies confirming that cytoplasmic droplets are replete with enzymes involved in energy metabolism (Yuan et al., 2013). Notably, proteins mapping to metabolic cascades such as oxidative phosphorylation, cholesterol biosynthesis, and fatty acid β-oxidation featured prominently among those identified as being lost by the maturing spermatozoa in the present study. Together, these data support previous claims that cytoplasmic droplets may serve as an energy-producing entity capable of fueling the molecular and cellular events underpinning epididymal sperm maturation (Yuan et al., 2013). Notably, however, the retention of cytoplasmic droplets in ejaculated spermatozoa has been negatively correlated with sperm fertility in both animals and humans (Cooper, 2011; Moore et al., 2010; Pena et al., 2007; Thundathil et al., 2001), indicating that the liberation of their spent payload of fuel reserves is also an important feature of epididymal maturation. Indeed, ejaculated spermatozoa of domestic animals containing a high proportion of proximally located cytoplasmic droplets are correlated with impaired *in vitro* fertilization (IVF) and artificial insemination

Table 2. Protein abundance changes associated with sperm capacitation

Accession	Protein name	Gene symbol	Fold change	p value
P52480	Pyruvate kinase PKM	*Pkm*	4.65	0.00001
Q9D1C8	Vacuolar protein sorting-associated protein 28 homolog	*Vps28*	3.88	0.00183
Q8VD04	GRIP1-associated protein 1	*Gripap1*	3.82	0.00010
P62257	Ubiquitin-conjugating enzyme E2 H	*Ube2h*	3.70	0.00047
Q7TMM9	Tubulin beta-2A chain	*Tubb2a*	3.13	0.00034
Q3ULW6-3	Isoform 3 of coiled-coil domain-containing protein 33	*Ccdc33*	3.08	0.00003
Q91YP3	Deoxyribose-phosphate aldolase	*Dera*	2.84	0.01147
P62313	U6 snRNA-associated Sm-like protein LSm6	*Lsm6*	2.64	0.00018
P16381	Putative ATP-dependent RNA helicase Pl10	*D1Pas1*	2.59	0.00015
Q07133	Histone H1t	*H1-6*	2.51	0.00009
Q80YW5	B box and SPRY domain-containing protein	*Bspry*	2.40	0.00079
Q8R2U0	Nucleoporin SEH1	*Seh1l*	2.34	0.00005
Q8VC16	Leucine-rich repeat-containing protein 14	*Lrrc14*	2.33	0.03901
P61079	Ubiquitin-conjugating enzyme E2 D3	*Ube2d3*	2.15	0.00002
E9Q557	Desmoplakin	*Dsp*	2.09	0.01415
Q9Z0U1	Tight junction protein ZO-2	*Tjp2*	2.07	0.00656
Q8VDN2	Sodium/potassium-transporting ATPase subunit alpha-1	*Atp1a1*	2.05	0.02131
O55142	60S ribosomal protein L35a	*Rpl35a*	2.05	0.00008
Q8BP48	Methionine aminopeptidase 1	*Metap1*	2.04	0.00011
Q9CWF2	Tubulin beta-2B chain	*Tubb2b*	−2.08	0.00002
Q7TPM3	E3 ubiquitin-protein ligase TRIM17	*Trim17*	−2.13	0.00006
Q9WTI7	Unconventional myosin-Ic	*Myo1c*	−2.22	0.00294
P62259	14-3-3 protein epsilon	*Ywhae*	−2.33	0.00006
Q9D3S5	NADP-dependent oxidoreductase domain-containing protein 1	*Noxred1*	−2.44	0.00811
Q60668	Heterogeneous nuclear ribonucleoprotein D0	*Hnrnpd*	−2.44	0.00049
Q62261	Spectrin beta chain, non-erythrocytic 1	*Sptbn1*	−3.03	0.00346
P07978	Protamine-2	*Prm2*	−5.56	0.00303
Q61165	Sodium/hydrogen exchanger 1	*Slc9a1*	−6.67	0.00002
Q99NB9	Splicing factor 3B subunit 1	*Sf3b1*	−6.67	0.00185

outcomes (Amann et al., 2000; Pena et al., 2007; Thundathil et al., 2001). Similarly, the presence of cytoplasmic droplets on ejaculated human spermatozoa has been linked with poor IVF and intracytoplasmic sperm injection outcomes (Cooper, 2005). Collectively, the data collated in our manuscript challenge the traditional view of the transformation of the maturing sperm cell being dominated by newly acquired proteins, revealing instead that the loss of proteins may be equally important to prime spermatozoa for motility and fertility competence.

Notwithstanding the unexpected finding that changes to the maturing sperm proteome are dominated by protein losses, these changes did occur in parallel with increased abundance and/or the new acquisition of a substantial number of proteins (i.e., 57 and 264 proteins, respectively), as many as 82% of which have previously been reported as being expressed in the mouse epididymal epithelial transcriptome (Johnston et al., 2005) (Table S4). These additions to the cauda epididymal sperm proteome could have a profound effect on their functional maturation, as suggested by the predicted activation of fertilization and, more specifically, cell movement and capacitation pathways; changes that appear to be linked with the increased abundance of a subset of at least 28 proteins. Prominent among the proteins associated with these pathways were ADCY10, cation channel sperm-associated protein 1, CFAP proteins 44, 65, and 157, and platelet-activating factor acetylhydrolase. In the absence of *de novo* protein translation, a prime candidate for mediating the bulk exchange of such proteomic information to maturing spermatozoa are epididymosomes, a heterogeneous population of small membrane bound extracellular vesicles (EVs) (Tamessar et al., 2021; Zhou et al., 2018) that are secreted from the lining epididymal epithelium (Sullivan, 2015; Tamessar et al., 2021; Zhou et al., 2018). This form of intercellular communication is initiated by the formation of

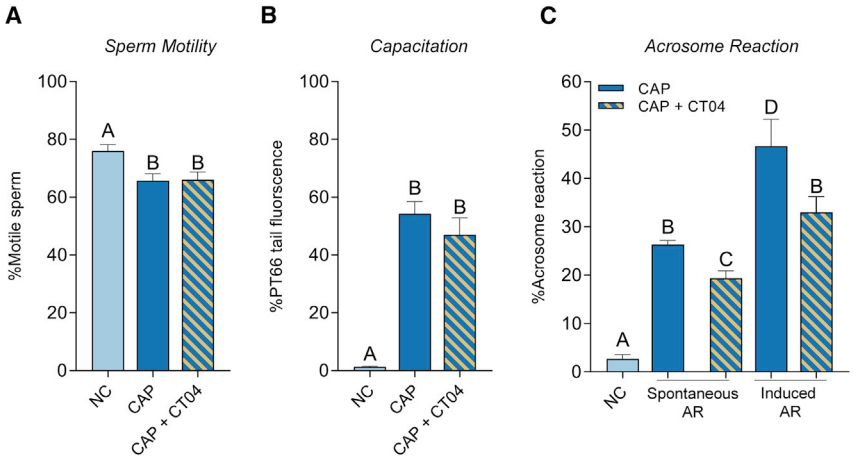

Figure 5. Inhibition of RHOA leads to an inhibition of the acrosome reaction

(A) Motility counts of spermatozoa from populations of non-capacitated, capacitated, and capacitated in presence of RHOA inhibitor CT04, which showed no decrease in percentage of motile sperm due to the inhibitor.

(B) Capacitation of these sperm populations was measured by phosphotyrosine immunofluorescence (PT66) and counting the percentage of sperm with tail fluorescence.

(C) The proficiency of the spermatozoa to acrosome react in the presence of CT04, either spontaneously or induced with A23187 calcium ionophore, was examined using PNA-FITC acrosome marker.

multivesicular bodies and the subsequent disbursement of their contents via cytoplasmic protrusions that form along the apical margin of the epididymal epithelial cells (Hermo and Jacks, 2002). Downstream of their release, epididymosomes have been shown to dock and transiently fuse with spermatozoa within the luminal environment of the epididymal tubule, thus enabling the transfer of a complex cargo comprising lipids, nucleic acids, and proteins to these recipient cells (Sullivan, 2015; Trigg et al., 2019; Zhou et al., 2018). Indeed, profiling of epididymosomes has revealed that their macromolecular composition is surprisingly complex, particularly given their relatively simple structure, indicating that these epididymis-specific vesicles likely play a central role in facilitating the remodeling of the sperm architecture (Trigg et al., 2019). Accordingly, 88% of the proteomic inventory previously identified in mouse epididymosomes (i.e., 1,445 out of 1,640 proteins) were also represented in the epididymal sperm proteome curated herein. This conservation included some 466 proteins that were only detected in caput epididymal sperm and a further 21 proteins that were uniquely detected in cauda epididymal sperm. Curiously, among the 927 epididymosome proteins shared between caput and cauda epididymal sperm, only seven proteins were significantly accumulated into cauda epididymal sperm, while 462 epididymosome proteins displayed the reciprocal trend of being underrepresented in the mature sperm population. Such findings raise the intriguing prospect that the temporary membrane continuity established during epididymosome-sperm interaction (Zhou et al., 2019) may facilitate bidirectional protein transfer, not only enabling the epididymosomes to expel fertilization related proteins, but also to sequester redundant/inhibitory proteins. In conjunction with the shedding of the cytoplasmic droplet (discussed above), this putative "kiss-and-run" mechanism of epididymosome-sperm interaction could contribute to the marked reduction in the overall complexity of the mature sperm proteome. While definitive evidence is required to substantiate this transformational potential of epididymosomes, it is perhaps notable that 99 sperm proteins that were identified as being lost/underrepresented in mature cauda epididymal sperm were in fact more abundant in the epididymosomes isolated from the same epididymal region (Nixon et al., 2019b).

Against the background of the overt proteomic changes associated with the acquisition of fertilization potential during epididymal maturation, we detected relatively modest additional changes linked to the realization of this potential in cells driven to capacitate *in vitro*. Indeed, only 19 and 10 proteins met the respective criteria for being over- or underrepresented in capacitated cauda epididymal sperm compared with that of their non-capacitated counterparts. These data agree with the notion that capacitation-associated priming of the translationally inert spermatozoon is primarily attributed to post-translational modification, unmasking, and/or repositioning of key elements of the intrinsic sperm proteome (Aitken and Nixon, 2013; Nixon et al., 2020), changes that could conceivably influence their efficiency of solubilization/extraction and hence differential abundance in capacitated vs. non-capacitated spermatozoa. Notably in this regard, we have shown that the stringency of cell lysis buffer and extraction technique does indeed influence the efficacy of sperm protein recovery (Figure S4A). Alternatively, those proteins underrepresented in the capacitated sperm population add to a growing list of putative decapacitation factors that are capable of stabilizing the spermatozoon and/or rendering them refractory to premature capacitation, compatible with their prolonged storage in the epididymis (Fraser, 2010; Nixon et al., 2006, 2020). By way of illustration, one such protein whose abundance was significantly reduced in capacitated spermatozoa (FC = −3.03) was spectrin beta chain, non-erythrocytic 1 (SPTBN1), a molecular scaffold capable of linking the plasma membrane to the actin cytoskeleton and thereby acting as a critical determinant of membrane integrity and the organization of integral proteins immersed within it (Bogusławska et al., 2014; Bose and Chakrabarti, 2020; Yang et al., 2021). Indeed, analogous with the role of spectrin in erythrocytes, it is tempting to speculate that this protein may form a component of the proteinaceous membrane skeleton that permits spermatozoa to withstand and respond to the mechanical stresses the cells experience during their journey to the site of fertilization. Moreover, the interaction of spectrin with a multitude of membrane channels, adhesion molecules, receptors, and transporters paints a picture of this multifunctional protein (Machnicka et al., 2019) as a potential interface for signal transduction events such as those involved in the initiation of capacitation (Nixon and Bromfield, 2018). Of particular relevance,

spectrin is known to interact with calmodulin and is thus a candidate for regulation of the calcium-dependent events that support sperm motility and fertilizing ability (Leclerc et al., 2020). At present it remains uncertain whether the capacitation-associated loss of spectrin is a cause or consequence of membrane remodeling, yet this remains an interesting avenue for future research.

Notably, in seeking to account for changes in the sperm proteome that link epididymal sperm maturation with the functional competence to engage in productive capacitation, we elected to focus on RHOA-mediated signaling pathways. The rational for this decision rests with the identification that RHOA experiences of gradient of increasing abundance between populations of caput and cauda epididymal spermatozoa, along with a wealth of somatic cell literature implicating RHOA in the regulation of actin dynamics (Kilian et al., 2021). However, unlike the mechanical influence exerted by spectrin, RHOA acts directly via a signaling cascade involving RHO kinase (ROCK), LIM kinase (LIMK), and cofilin. The activity of this RHOA-ROCK-LIMK-cofilin pathway appears to be conserved in spermatozoa of species such as the bovine (Fiedler et al., 2008), mouse (Romarowski et al., 2015), and guinea pig (Reyes-Miguel et al., 2020), wherein RHOA has been implicated in the regulation of actin polymerization events that precede the induction of acrosomal exocytosis. Accordingly, herein we demonstrated that selective pharmacological inhibition of RHOA led to a significant decrease in both spontaneous and induced acrosome reaction rates that occurred independent of an attendant loss of sperm viability. We also demonstrated that numerous interacting proteins that are capable of repressing RHOA activity are either significantly downregulated or completely lost from the proteome of cauda epididymal sperm. Together, these data suggest that the absence and/or suppression of the activity of key intermediary protein signaling machinery may, at least in part, account for the fact that immature caput epididymal sperm are refractory to capacitation-inducing stimuli. Support for this notion rests with independent evidence that sperm transit through the mouse epididymis has also been linked to the acquisition of cSRC (Krapf et al., 2012), a tyrosine kinase that drives important aspects of capacitation-associated signaling (Baker et al., 2006; Mitchell et al., 2008; Stival et al., 2015). Moreover, our own data identified at least 14 kinases among those proteins that are either newly acquired or increase in abundance coincident with epididymal sperm maturation. Similar to cSRC (Krapf et al., 2012), three of these kinases are enriched in epididymosomes (Nixon et al., 2019b), further implicating these vesicles in the trafficking of fertilization-related proteins to the maturing sperm cell.

In summary, the epididymal sperm proteomes characterized in this study advance our understanding of sperm cell biology and shed light on the extent of the proteomic changes that accompany the functional maturation of these cells. Indeed, contrary to the long-held belief that epididymal maturation is primarily driven by the uptake/modification of additional proteins, our data demonstrates that spermatozoa shed over half their protein composition during this process. Moreover, these data suggest that the consequences of retaining proteins that should otherwise be shed may be equally as detrimental to sperm function as failing to acquire specific proteins during epididymal transit. This improved understanding of sperm cell biology demonstrates the level of evolutionary complexity invested in epididymal maturation and provides a platform from which to identify key proteins that are essential for fertilization. We envision the most immediate clinical impact of this work will be on the detection of defects in sperm maturation causally associated with male infertility. As an additional dividend, with increasing recognition that male reproductive health is inextricably linked to overall health, and that poor semen parameters have utility as a "canary in the coal mine" foreshadowing the onset of a spectrum of co-morbidities (Burke et al., 2022), the proteomic resources provided here may find application in the prediction of the long-term health of individuals.

Limitations of the study

This study has exploited high-resolution, label-free quantitative MS to generate a detailed inventory of the proteins comprising highly enriched populations of immature caput epididymal mouse spermatozoa and that of their non-capacitated and capacitated cauda epididymal sperm counterparts. Notwithstanding the molecular insights this study provides, we also draw attention to its limitations. Most notably, we are reticent to directly correlate changes in the abundance of any given protein with either its function or its overall activity in spermatozoa. This issue applies equally in the context of both epididymal maturation and the subsequent induction of capacitation, whereby we caution that changes in protein levels associated with either event should not be interpreted as direct, substantiating evidence of their involvement in the regulation of these biological processes. Therefore, in addition to the use of *in silico* algorithms to predict the activation of protein signaling pathways, we stress the importance of performing orthogonal functional analyses on selected proteins (such as those reported herein for RHOA) to validate their contribution to the functional transformation of spermatozoa. In a similar context, we also advocate for the use of complementary MS techniques and functional assays to study the extent of post-translational modifications (PTMs) that accompany the changes in the core proteome of maturing spermatozoa. Indeed, of the more than 200 known forms of PTM (Walsh et al., 2005), transient protein phosphorylation has emerged as one of the major regulators of sperm function, having previously been implicated in sperm cell metabolism, signaling, and modifications of the sperm membrane architecture (Aitken and Nixon, 2013; Gervasi and Visconti, 2016). Beyond the merits of functional analyses, we also emphasize that we have not demonstrated the mechanisms responsible for such substantial modification of the sperm proteome. While we have speculated at the importance of cytoplasmic droplet shedding and EVs for mediation of bulk changes, alternative explanations include differences in the solubilization and extraction efficiency of select proteins, and although it is contrary to central dogma, we do also acknowledge studies purporting that spermatozoa may possess limited ability to translate nuclear-encoded proteins via mitochondrial-type ribosomes (Gur and Breitbart, 2006). Resolving such issues may ultimately benefit from a more detailed temporal knowledge of the sequential sperm proteome changes occurring along the length of the epididymal tract. In this regard,

transcriptomic profiling studies of the mouse epididymis have identified no fewer than six distinct transcriptional units (Johnston et al., 2005), while the application of MALDI imaging MS has revealed 24 and 22 zones possessing discrete molecular signatures in the rat epididymis (Lagarrigue et al., 2020). Clearly, we still have much ground to cover in terms of defining the unique molecular signatures responsible for supporting the progressive development of post-testicular sperm maturation.

STAR★METHODS

Detailed methods are provided in the online version of this paper and include the following:

- KEY RESOURCES TABLE
- RESOURCE AVAILABILITY
  - Lead contact
  - Materials availability
  - Data and code availability
- EXPERIMENTAL MODEL AND SUBJECT DETAILS
  - Ethics approval
- METHOD DETAILS
  - Isolation of epididymal spermatozoa
  - Proteomic sample preparation of spermatozoa
  - nLC-MS/MS analysis
  - Immunofluorescence
  - SDS-PAGE and immunoblotting
  - RHOA inhibition studies
- QUANTIFICATION AND STATISTICAL ANALYSIS
  - Proteomic data processing and analysis
  - Ingenuity pathway analysis and phenotype comparison
  - Immunoblot densitometry
- STATISTICAL ANALYSIS

SUPPLEMENTAL INFORMATION

Supplemental information can be found online at https://doi.org/10.1016/j.celrep.2022.111655.

ACKNOWLEDGMENTS

We thank Dr. Ben Crossett and Jens Altvater from the Mass Spectrometry Core Facility at The University of Sydney, Nathan Smith from The University of Newcastle Analytical Biomolecular Research Facility (ABRF), and the Academic and Research Computing Support team, The University of Newcastle who provided High Performance Computing Infrastructure to support the bioinformatics analyses. This research was supported by a National Health and Medical Research Council (NHMRC) of Australia Project Grant awarded to B.N. and M.D.D. (APP1147932). B.N., E.G.B., and M.D.D. are recipients of NHMRC Research Fellowships.

AUTHOR CONTRIBUTIONS

Conceptualization, D.A.S.B. and B.N.; methodology, D.A.S.B., S.J.H., and B.N.; investigation, D.A.S.B., A.L.A., I.R.B., and S.J.H.; formal analysis, D.A.S.B. and B.N.; validation, D.A.S.B., A.L.A., I.R.B., and J.E.M.; writing – original draft, D.A.S.B. and B.N.; writing – review & editing, D.A.S.B., A.L.A., E.G.B., I.R.B., J.E.M., J.E.S., M.D.D., S.J.H., and B.N.; funding acquisition, B.N. and M.D.D.; resources, S.J.H. and B.N.; supervision, B.N.

DECLARATION OF INTERESTS

The authors declare no competing interests.

Received: October 6, 2021
Revised: June 15, 2022
Accepted: October 20, 2022
Published: November 15, 2022

REFERENCES

Aitken, R.J., and Nixon, B. (2013). Sperm capacitation: a distant landscape glimpsed but unexplored. Mol. Hum. Reprod. *19*, 785–793. https://doi.org/10.1093/molehr/gat067.

Aitken, R.J., Nixon, B., Lin, M., Koppers, A.J., Lee, Y.H., and Baker, M.A. (2007). Proteomic changes in mammalian spermatozoa during epididymal maturation. Asian J. Androl. *9*, 554–564. https://doi.org/10.1111/j.1745-7262.2007.00280.x.

Amann, R.P., Seidel, G.E., Jr., and Mortimer, R.G. (2000). Fertilizing potential in vitro of semen from young beef bulls containing a high or low percentage of sperm with a proximal droplet. Theriogenology *54*, 1499–1515. https://doi.org/10.1016/s0093-691x(00)00470-2.

Amaral, A., Castillo, J., Ramalho-Santos, J., and Oliva, R. (2014 Jan-Feb). The combined human sperm proteome: cellular pathways and implications for basic and clinical science. Hum. Reprod. Update *20*, 40–62. https://doi.org/10.1093/humupd/dmt046.

Anderson, A.L., Stanger, S.J., Mihalas, B.P., Tyagi, S., Holt, J.E., McLaughlin, E.A., and Nixon, B. (2015). Assessment of microRNA expression in mouse epididymal epithelial cells and spermatozoa by next generation sequencing. Genom. Data *6*, 208–211. https://doi.org/10.1016/j.gdata.2015.09.012.

Asquith, K.L., Baleato, R.M., McLaughlin, E.A., Nixon, B., and Aitken, R.J. (2004). Tyrosine phosphorylation activates surface chaperones facilitating sperm-zona recognition. J. Cell Sci. *117*, 3645–3657. https://doi.org/10.1242/jcs.01214.

Au, C.E., Hermo, L., Byrne, E., Smirle, J., Fazel, A., Kearney, R.E., Smith, C.E., Vali, H., Fernandez-Rodriguez, J., Simon, P.H.G., et al. (2015). Compartmentalization of membrane trafficking, glucose transport, glycolysis, actin, tubulin and the proteasome in the cytoplasmic droplet/Hermes body of epididymal sperm. Open Biol. *5*, 150080.

Baker, M.A., Hetherington, L., and Aitken, R.J. (2006). Identification of SRC as a key PKA-stimulated tyrosine kinase involved in the capacitation-associated hyperactivation of murine spermatozoa. J. Cell Sci. *119*, 3182–3192. https://doi.org/10.1242/jcs.03055.

Baker, M.A., Nixon, B., Naumovski, N., and Aitken, R.J. (2012). Proteomic insights into the maturation and capacitation of mammalian spermatozoa. Syst. Biol. Reprod. Med. *58*, 211–217. https://doi.org/10.3109/19396368.2011.639844.

Bedford, J.M. (2015). The epididymis re-visited: a personal view. Asian J. Androl. *17*, 693–698. https://doi.org/10.4103/1008-682x.153297.

Bogusławska, D.M., Machnicka, B., Hryniewicz-Jankowska, A., and Czogalla, A. (2014). Spectrin and phospholipids - the current picture of their fascinating interplay. Cell. Mol. Biol. Lett. *19*, 158–179. https://doi.org/10.2478/s11658-014-0185-5.

Bose, D., and Chakrabarti, A. (2020). Multiple functions of spectrin: convergent effects. J. Membr. Biol. *253*, 499–508. https://doi.org/10.1007/s00232-020-00142-1.

Burke, N.D., Nixon, B., Roman, S.D., Schjenken, J.E., Walters, J.L.H., Aitken, R.J., and Bromfield, E.G. (2022). Male infertility and somatic health - insights into lipid damage as a mechanistic link. Nat. Rev. Urol. https://doi.org/10.1038/s41585-022-00640-y.

Caballero, J.N., Frenette, G., Belleannée, C., and Sullivan, R. (2013). CD9-positive microvesicles mediate the transfer of molecules to Bovine Spermatozoa during epididymal maturation. PLoS One *8*, e65364. https://doi.org/10.1371/journal.pone.0065364.

Cafe, S.L., Nixon, B., Dun, M.D., Roman, S.D., Bernstein, I.R., and Bromfield, E.G. (2020). Oxidative stress dysregulates protein homeostasis within the male germ line. Antioxid. Redox Signal. *32*, 487–503. https://doi.org/10.1089/ars.2019.7832.

Cayli, S., Jakab, A., Ovari, L., Delpiano, E., Celik-Ozenci, C., Sakkas, D., Ward, D., and Huszar, G. (2003). Biochemical markers of sperm function: male fertility and sperm selection for ICSI. Reprod. Biomed. Online *7*, 462–468. https://doi.org/10.1016/s1472-6483(10)61891-3.

Cooper, T.G. (2005). Cytoplasmic droplets: the good, the bad or just confusing? Hum. Reprod. *20*, 9–11. https://doi.org/10.1093/humrep/deh555.

Cooper, T.G. (2011). The epididymis, cytoplasmic droplets and male fertility. Asian J. Androl. *13*, 130–138. https://doi.org/10.1038/aja.2010.97.

Degryse, S., de Bock, C.E., Demeyer, S., Govaerts, I., Bornschein, S., Verbeke, D., Jacobs, K., Binos, S., Skerrett-Byrne, D.A., Murray, H.C., et al. (2018). Mutant JAK3 phosphoproteomic profiling predicts synergism between JAK3 inhibitors and MEK/BCL2 inhibitors for the treatment of T-cell acute lymphoblastic leukemia. Leukemia *32*, 788–800. https://doi.org/10.1038/leu.2017.276.

Dickinson, M.E., Flenniken, A.M., Ji, X., Teboul, L., Wong, M.D., White, J.K., Meehan, T.F., Weninger, W.J., Westerberg, H., Adissu, H., et al. (2016). High-throughput discovery of novel developmental phenotypes. Nature *537*, 508–514. https://doi.org/10.1038/nature19356.

Dott, H.M., and Dingle, J.T. (1968). Distribution of lysosomal enzymes in the spermatozoa and cytoplasmic droplets of bull and ram. Exp. Cell Res. *52*, 523–540. https://doi.org/10.1016/0014-4827(68)90493-x.

Dun, M.D., Anderson, A.L., Bromfield, E.G., Asquith, K.L., Emmett, B., McLaughlin, E.A., Aitken, R.J., and Nixon, B. (2012). Investigation of the expression and functional significance of the novel mouse sperm protein, a disintegrin and metalloprotease with thrombospondin type 1 motifs number 10 (ADAMTS10). Int. J. Androl. *35*, 572–589. https://doi.org/10.1111/j.1365-2605.2011.01235.x.

Dun, M.D., Mitchell, L.A., Aitken, R.J., and Nixon, B. (2010). Sperm-zona pellucida interaction: molecular mechanisms and the potential for contraceptive intervention. Handb. Exp. Pharmacol. *139*, 139–178. https://doi.org/10.1007/978-3-642-02062-9_9.

Ergur, A.R., Dokras, A., Giraldo, J.L., Habana, A., Kovanci, E., and Huszar, G. (2002). Sperm maturity and treatment choice of in vitro fertilization (IVF) or intracytoplasmic sperm injection: diminished sperm HspA2 chaperone levels predict IVF failure. Fertil. Steril. *77*, 910–918. https://doi.org/10.1016/s0015-0282(02)03073-x.

Esposito, G., Jaiswal, B.S., Xie, F., Krajnc-Franken, M.A.M., Robben, T.J.A.A., Strik, A.M., Kuil, C., Philipsen, R.L.A., van Duin, M., Conti, M., et al. (2004). Mice deficient for soluble adenylyl cyclase are infertile because of a severe sperm-motility defect. Proc. Natl. Acad. Sci. USA *101*, 2993–2998. https://doi.org/10.1073/pnas.0400050101.

Fiedler, S.E., Bajpai, M., and Carr, D.W. (2008). Identification and characterization of RHOA-interacting proteins in bovine Spermatozoa1. Biol. Reprod. *78*, 184–192. https://doi.org/10.1095/biolreprod.107.062943.

Fraser, L.R. (2010). The "switching on" of mammalian spermatozoa: molecular events involved in promotion and regulation of capacitation. Mol. Reprod. Dev. *77*, 197–208.

Garbers, D.L., Wakabayashi, T., and Reed, P.W. (1970). Enzyme profile of the cytoplasmic droplet from bovine epididymal spermatozoa. Biol. Reprod. *3*, 327–337. https://doi.org/10.1093/biolreprod/3.3.327.

Gervasi, M.G., and Visconti, P.E. (2016). Chang's meaning of capacitation: a molecular perspective. Mol. Reprod. Dev. *83*, 860–874. https://doi.org/10.1002/mrd.22663.

Gur, Y., and Breitbart, H. (2006). Mammalian sperm translate nuclear-encoded proteins by mitochondrial-type ribosomes. Genes Dev. *20*, 411–416. https://doi.org/10.1101/gad.367606.

Harrison, R.A., and White, I.G. (1972). Glycolytic enzymes in the spermatozoa and cytoplasmic droplets of bull, boar and ram, and their leakage afte shock. J. Reprod. Fertil. *30*, 105–115. https://doi.org/10.1530/jrf.0.0300105.

Hermo, L., and Jacks, D. (2002). Nature's ingenuity: bypassing the classical secretory route via apocrine secretion. Mol. Reprod. Dev. *63*, 394–410. https://doi.org/10.1002/mrd.90023.

Hermo, L., Oliveira, R.L., Smith, C.E., Au, C.E., and Bergeron, J.J.M. (2019). Dark side of the epididymis: tails of sperm maturation. Andrology *7*, 566–580. https://doi.org/10.1111/andr.12641.

Hermo, L., Pelletier, R.M., Cyr, D.G., and Smith, C.E. (2010a). Surfing the wave, cycle, life history, and genes/proteins expressed by testicular germ cells. Part 1: background to spermatogenesis, spermatogonia, and spermatocytes. Microsc. Res. Tech. *73*, 241–278. https://doi.org/10.1002/jemt.20783.

Hermo, L., Pelletier, R.M., Cyr, D.G., and Smith, C.E. (2010b). Surfing the wave, cycle, life history, and genes/proteins expressed by testicular germ cells. Part 2: changes in spermatid organelles associated with development of spermatozoa. Microsc. Res. Tech. *73*, 279–319. https://doi.org/10.1002/jemt.20787.

Humphrey, S.J., Karayel, O., James, D.E., and Mann, M. (2018). High-throughput and high-sensitivity phosphoproteomics with the EasyPhos platform. Nat. Protoc. *13*, 1897–1916.

Hutcheon, K., McLaughlin, E.A., Stanger, S.J., Bernstein, I.R., Dun, M.D., Eamens, A.L., and Nixon, B. (2017). Analysis of the small non-protein-coding RNA profile of mouse spermatozoa reveals specific enrichment of piRNAs within mature spermatozoa. RNA Biol. *14*, 1776–1790. https://doi.org/10.1080/15476286.2017.1356569.

Johnston, D.S., Jelinsky, S.A., Bang, H.J., DiCandeloro, P., Wilson, E., Kopf, G.S., and Turner, T.T. (2005). The mouse epididymal transcriptome: transcriptional profiling of segmental gene expression in the epididymis. Biol. Reprod. *73*, 404–413. https://doi.org/10.1095/biolreprod.105.039719.

Kilian, L.S., Voran, J., Frank, D., and Rangrez, A.Y. (2021). RhoA: a dubious molecule in cardiac pathophysiology. J. Biomed. Sci. *28*, 33. 21.

Krämer, A., Green, J., Pollard, J., Jr., and Tugendreich, S. (2014). Causal analysis approaches in ingenuity pathway analysis. Bioinformatics *30*, 523–530. https://doi.org/10.1093/bioinformatics/btt703.

Krapf, D., Ruan, Y.C., Wertheimer, E.V., Battistone, M.A., Pawlak, J.B., Sanjay, A., Pilder, S.H., Cuasnicu, P., Breton, S., and Visconti, P.E. (2012). cSrc is necessary for epididymal development and is incorporated into sperm during epididymal transit. Dev. Biol. *369*, 43–53. https://doi.org/10.1016/j.ydbio.2012.06.017.

Lagarrigue, M., Lavigne, R., Guével, B., Palmer, A., Rondel, K., Guillot, L., Kobarg, J.H., Trede, D., and Pineau, C. (2020). Spatial segmentation and metabolite annotation involved in sperm maturation in the rat epididymis by MALDI imaging mass spectrometry. J. Mass Spectrom. *55*, e4633. https://doi.org/10.1002/jms.4633.

Leclerc, P., Goupil, S., Rioux, J.F., Lavoie-Ouellet, C., Clark, M.È., Ruiz, J., and Saindon, A.A. (2020). Study on the role of calmodulin in sperm function through the enrichment and identification of calmodulin-binding proteins in bovine ejaculated spermatozoa. J. Cell. Physiol. *235*, 5340–5352.

Lee, L., Campagna, D.R., Pinkus, J.L., Mulhern, H., Wyatt, T.A., Sisson, J.H., Pavlik, J.A., Pinkus, G.S., and Fleming, M.D. (2008). Primary ciliary dyskinesia in mice lacking the novel ciliary protein Pcdp1. Mol. Cell Biol. *28*, 949–957. https://doi.org/10.1128/mcb.00354-07.

Machnicka, B., Grochowalska, R., Bogusławska, D.M., and Sikorski, A.F. (2019). The role of spectrin in cell adhesion and cell–cell contact. Exp. Biol. Med. *244*, 1303–1312. https://doi.org/10.1177/1535370219859003.

Maeda, M., Hasegawa, H., Hyodo, T., Ito, S., Asano, E., Yuang, H., Funasaka, K., Shimokata, K., Hasegawa, Y., Hamaguchi, M., and Senga, T. (2011). ARHGAP18, a GTPase-activating protein for RhoA, controls cell shape, spreading, and motility. Mol. Biol. Cell *22*, 3840–3852. https://doi.org/10.1091/mbc.E11-04-0364.

McKenzie, C.W., and Lee, L. (2020). Genetic interaction between central pair apparatus genes CFAP221, CFAP54, and SPEF2 in mouse models of primary ciliary dyskinesia. Sci. Rep. *10*, 12337. https://doi.org/10.1038/s41598-020-69359-3.

Mitchell, L.A., Nixon, B., Baker, M.A., and Aitken, R.J. (2008). Investigation of the role of SRC in capacitation-associated tyrosine phosphorylation of human spermatozoa. Mol. Hum. Reprod. *14*, 235–243. https://doi.org/10.1093/molehr/gan007.

Moore, K., Lovercamp, K., Feng, D., Antelman, J., Sutovsky, M., Manandhar, G., van Leyen, K., Safranski, T., and Sutovsky, P. (2010). Altered epididymal sperm maturation and cytoplasmic droplet migration in subfertile male Alox15 mice. Cell Tissue Res. *340*, 569–581. https://doi.org/10.1007/s00441-010-0972-x.

Murray, H.C., Enjeti, A.K., Kahl, R.G.S., Flanagan, H.M., Sillar, J., Skerrett-Byrne, D.A., Al Mazi, J.G., Au, G.G., de Bock, C.E., Evans, K., et al. (2021). Quantitative phosphoproteomics uncovers synergy between DNA-PK and FLT3 inhibitors in acute myeloid leukaemia. Leukemia *35*, 1782–1787. https://doi.org/10.1038/s41375-020-01050-y.

Naaby-Hansen, S., Mandal, A., Wolkowicz, M.J., Sen, B., Westbrook, V.A., Shetty, J., Coonrod, S.A., Klotz, K.L., Kim, Y.H., Bush, L.A., et al. (2002). CABYR, a novel calcium-binding tyrosine phosphorylation-regulated fibrous sheath protein involved in capacitation. Dev. Biol. *242*, 236–254. https://doi.org/10.1006/dbio.2001.0527.

Nixon, B., and Bromfield, E.G. (2018). Sperm capacitation. In Encyclopedia of Reproduction, Second Edition, M.K. Skinner, ed. (Academic Press), pp. 272–278. https://doi.org/10.1016/B978-0-12-801238-3.64464-1.

Nixon, B., Bromfield, E.G., Cui, J., and De Iuliis, G.N. (2017). Heat shock protein A2 (HSPA2): regulatory roles in germ cell development and sperm function. Adv. Anat. Embryol. Cell Biol. *222*, 67–93. https://doi.org/10.1007/978-3-319-51409-3_4.

Nixon, B., Bromfield, E.G., Dun, M.D., Redgrove, K.A., McLaughlin, E.A., and Aitken, R.J. (2015a). The role of the molecular chaperone heat shock protein A2 (HSPA2) in regulating human sperm-egg recognition. Asian J. Androl. *17*, 568–573. https://doi.org/10.4103/1008-682x.151395.

Nixon, B., Cafe, S.L., Eamens, A.L., De Iuliis, G.N., Bromfield, E.G., Martin, J.H., Skerrett-Byrne, D.A., and Dun, M.D. (2020). Molecular insights into the divergence and diversity of post-testicular maturation strategies. Mol. Cell. Endocrinol. *517*, 110955. https://doi.org/10.1016/j.mce.2020.110955.

Nixon, B., De Iuliis, G.N., Dun, M.D., Zhou, W., Trigg, N.A., and Eamens, A.L. (2019a). Profiling of epididymal small non-protein-coding RNAs. Andrology *7*, 669–680. https://doi.org/10.1111/andr.12640.

Nixon, B., De Iuliis, G.N., Hart, H.M., Zhou, W., Mathe, A., Bernstein, I.R., Anderson, A.L., Stanger, S.J., Skerrett-Byrne, D.A., Jamaluddin, M.F.B., et al. (2019b). Proteomic profiling of mouse epididymosomes reveals their contributions to post-testicular sperm maturation. Mol. Cell. Proteomics *18*, S91–S108. https://doi.org/10.1074/mcp.RA118.000946.

Nixon, B., Johnston, S.D., Skerrett-Byrne, D.A., Anderson, A.L., Stanger, S.J., Bromfield, E.G., Martin, J.H., Hansbro, P.M., and Dun, M.D. (2019c). Modification of crocodile spermatozoa refutes the tenet that post-testicular sperm maturation is restricted to mammals. Mol. Cell. Proteomics *18*, S58–S76. https://doi.org/10.1074/mcp.RA118.000904.

Nixon, B., MacIntyre, D.A., Mitchell, L.A., Gibbs, G.M., O'Bryan, M., and Aitken, R.J. (2006). The identification of mouse sperm-surface-associated proteins and characterization of their ability to act as decapacitation factors. Biol. Reprod. *74*, 275–287. https://doi.org/10.1095/biolreprod.105.044644.

Nixon, B., Stanger, S.J., Mihalas, B.P., Reilly, J.N., Anderson, A.L., Dun, M.D., Tyagi, S., Holt, J.E., and McLaughlin, E.A. (2015b). Next generation sequencing analysis reveals segmental patterns of microRNA expression in mouse epididymal epithelial cells. PLoS One *10*, e0135605. https://doi.org/10.1371/journal.pone.0135605.

Nixon, B., Stanger, S.J., Mihalas, B.P., Reilly, J.N., Anderson, A.L., Tyagi, S., Holt, J.E., and McLaughlin, E.A. (2015c). The microRNA signature of mouse spermatozoa is substantially modified during epididymal maturation. Biol. Reprod. *93*, 91. https://doi.org/10.1095/biolreprod.115.132209.

Peña, A.I., Barrio, M., Becerra, J.J., Quintela, L.A., and Herradón, P.G. (2007). Infertility in a dog due to proximal cytoplasmic droplets in the ejaculate: investigation of the significance for sperm functionality in vitro. Reprod. Domest. Anim. *42*, 471–478. https://doi.org/10.1111/j.1439-0531.2006.00809.x.

Perez-Riverol, Y., Csordas, A., Bai, J., Bernal-Llinares, M., Hewapathirana, S., Kundu, D.J., Inuganti, A., Griss, J., Mayer, G., Eisenacher, M., et al. (2019). The PRIDE database and related tools and resources in 2019: improving support for quantification data. Nucleic Acids Res. *47*, D442–D450. https://doi.org/10.1093/nar/gky1106.

Rappsilber, J., Mann, M., and Ishihama, Y. (2007). Protocol for micro-purification, enrichment, pre-fractionation and storage of peptides for proteomics using StageTips. Nat. Protoc. *2*, 1896–1906. https://doi.org/10.1038/nprot.2007.261.

Redgrove, K.A., Nixon, B., Baker, M.A., Hetherington, L., Baker, G., Liu, D.Y., and Aitken, R.J. (2012). The molecular chaperone HSPA2 plays a key role in regulating the expression of sperm surface receptors that mediate sperm-egg recognition. PLoS One *7*, e50851. https://doi.org/10.1371/journal.pone.0050851.

Reid, A.T., Redgrove, K., Aitken, R.J., and Nixon, B. (2011). Cellular mechanisms regulating sperm-zona pellucida interaction. Asian J. Androl. *13*, 88–96. https://doi.org/10.1038/aja.2010.74.

Reyes-Miguel, T., Roa-Espitia, A.L., Baltiérrez-Hoyos, R., and Hernández-González, E.O. (2020). CDC42 drives RHOA activity and actin polymerization during capacitation. Reproduction *160*, 393–404. https://doi.org/10.1530/rep-19-0577.

Roberts, M.L., Scouten, W.H., and Nyquist, S.E. (1976). Isolation and characterization of the cytoplasmic droplet in the rat. Biol. Reprod. *14*, 421–424. https://doi.org/10.1095/biolreprod14.4.421.

Romarowski, A., Battistone, M.A., La Spina, F.A., Puga Molina, L.d.C., Luque, G.M., Vitale, A.M., Cuasnicu, P.S., Visconti, P.E., Krapf, D., and Buffone, M.G. (2015). PKA-dependent phosphorylation of LIMK1 and Cofilin is essential for mouse sperm acrosomal exocytosis. Dev. Biol. *405*, 237–249.

Schmid, A., Sutto, Z., Nlend, M.C., Horvath, G., Schmid, N., Buck, J., Levin, L.R., Conner, G.E., Fregien, N., and Salathe, M. (2007). Soluble adenylyl cyclase is localized to cilia and contributes to ciliary beat frequency regulation via production of cAMP. J. Gen. Physiol. *130*, 99–109. https://doi.org/10.1085/jgp.200709784.

Skerget, S., Rosenow, M.A., Petritis, K., and Karr, T.L. (2015). Sperm proteome maturation in the mouse epididymis. PLoS One *10*, e0140650. https://doi.org/10.1371/journal.pone.0140650.

Skerrett-Byrne, D.A., Anderson, A.L., Hulse, L., Wass, C., Dun, M.D., Bromfield, E.G., De Iuliis, G.N., Pyne, M., Nicolson, V., Johnston, S.D., and Nixon, B. (2021a). Proteomic analysis of koala (phascolarctos cinereus) spermatozoa and prostatic bodies. Proteomicse2100067. https://doi.org/10.1002/pmic.202100067.

Skerrett-Byrne, D.A., Bromfield, E.G., Murray, H.C., Jamaluddin, M.F.B., Jarnicki, A.G., Fricker, M., Essilfie, A.T., Jones, B., Haw, T.J., Hampsey, D., et al. (2021b). Time-resolved proteomic profiling of cigarette smoke-induced experimental chronic obstructive pulmonary disease. Respirology *26*, 960–973. https://doi.org/10.1111/resp.14111.

Skerrett-Byrne, D.A., Trigg, N.A., Bromfield, E.G., Dun, M.D., Bernstein, I.R., Anderson, A.L., Stanger, S.J., MacDougall, L.A., Lord, T., Aitken, R.J., et al. (2021c). Proteomic dissection of the impact of environmental exposures on mouse seminal vesicle function. Mol. Cell. Proteomics *20*, 100107. https://doi.org/10.1016/j.mcpro.2021.100107.

Smith, C.L., and Eppig, J.T. (2009). The mammalian phenotype ontology: enabling robust annotation and comparative analysis. Wiley Interdiscip. Rev. Syst. Biol. Med. *1*, 390–399. https://doi.org/10.1002/wsbm.44.

Smyth, S.P., Nixon, B., Anderson, A.L., Murray, H.C., Martin, J.H., Macdougall, L.A., Robertson, S.A., Skerrett-Byrne, D.A., and Schjenken, J.E. (2022). Elucidation of the protein composition of mouse seminal vesicle fluid. Proteomics *22*. https://doi.org/10.1002/pmic.202100227.

Stival, C., La Spina, F.A., Baró Graf, C., Arcelay, E., Arranz, S.E., Ferreira, J.J., Le Grand, S., Dzikunu, V.A., Santi, C.M., Visconti, P.E., et al. (2015). Src kinase is the connecting player between protein kinase A (PKA) activation and hyperpolarization through SLO3 potassium channel regulation in mouse sperm. J. Biol. Chem. *290*, 18855–18864. https://doi.org/10.1074/jbc.M115.640326.

Sullivan, R. (2015). Epididymosomes: a heterogeneous population of microvesicles with multiple functions in sperm maturation and storage. Asian J. Androl. *17*, 726–729. https://doi.org/10.4103/1008-682x.155255.

Tamessar, C.T., Trigg, N.A., Nixon, B., Skerrett-Byrne, D.A., Sharkey, D.J., Robertson, S.A., Bromfield, E.G., and Schjenken, J.E. (2021). Roles of male reproductive tract extracellular vesicles in reproduction. Am. J. Reprod. Immunol. *85*, e13338. https://doi.org/10.1111/aji.13338.

Tang, S., Wang, X., Li, W., Yang, X., Li, Z., Liu, W., Li, C., Zhu, Z., Wang, L., Wang, J., et al. (2017). Biallelic mutations in CFAP43 and CFAP44 cause male infertility with multiple morphological abnormalities of the sperm flagella. Am. J. Hum. Genet. *100*, 854–864. https://doi.org/10.1016/j.ajhg.2017.04.012.

Thundathil, J., Palasz, A.T., Barth, A.D., and Mapletoft, R.J. (2001). The use of in vitro fertilization techniques to investigate the fertilizing ability of bovine sperm with proximal cytoplasmic droplets. Anim. Reprod. Sci. *65*, 181–192. https://doi.org/10.1016/s0378-4320(00)00231-1.

Tollner, T.L., Yudin, A.I., Treece, C.A., Overstreet, J.W., and Cherr, G.N. (2004). Macaque sperm release ESP13.2 and PSP94 during capacitation: the absence of ESP13.2 is linked to sperm-zona recognition and binding. Mol. Reprod. Dev. *69*, 325–337. https://doi.org/10.1002/mrd.20132.

Trigg, N.A., Eamens, A.L., and Nixon, B. (2019). The contribution of epididymosomes to the sperm small RNA profile. Reproduction *157*, R209–R223.

Tyanova, S., Temu, T., Sinitcyn, P., Carlson, A., Hein, M.Y., Geiger, T., Mann, M., and Cox, J. (2016). The Perseus computational platform for comprehensive analysis of (prote)omics data. Nat. Methods *13*, 731–740. https://doi.org/10.1038/nmeth.3901.

Walsh, C.T., Garneau-Tsodikova, S., and Gatto, G.J., Jr. (2005). Protein posttranslational modifications: the chemistry of proteome diversifications. Angew. Chem. Int. Ed. Engl. *44*, 7342–7372. https://doi.org/10.1002/anie.200501023.

Yang, P., Yang, Y., Sun, P., Tian, Y., Gao, F., Wang, C., Zong, T., Li, M., Zhang, Y., Yu, T., and Jiang, Z. (2021). βII spectrin (SPTBN1): biological function and clinical potential in cancer and other diseases. Int. J. Biol. Sci. *17*, 32–49. https://doi.org/10.7150/ijbs.52375.

Yuan, S., Zheng, H., Zheng, Z., and Yan, W. (2013). Proteomic analyses reveal a role of cytoplasmic droplets as an energy source during epididymal sperm maturation. PLoS One *8*, e77466. https://doi.org/10.1371/journal.pone.0077466.

Yudin, A.I., Tollner, T.L., Treece, C.A., Kays, R., Cherr, G.N., Overstreet, J.W., and Bevins, C.L. (2008). Beta-defensin 22 is a major component of the mouse sperm glycocalyx. Reproduction *136*, 753–765. https://doi.org/10.1530/rep-08-0164.

Zheng, G., Dahl, J.A., Niu, Y., Fedorcsak, P., Huang, C.M., Li, C.J., Vågbø, C.B., Shi, Y., Wang, W.L., Song, S.H., et al. (2013). ALKBH5 is a mammalian RNA demethylase that impacts RNA metabolism and mouse fertility. Mol. Cell *49*, 18–29. https://doi.org/10.1016/j.molcel.2012.10.015.

Zhou, W., De Iuliis, G.N., Dun, M.D., and Nixon, B. (2018). Characteristics of the epididymal luminal environment responsible for sperm maturation and storage. Front. Endocrinol. *9*, 59. https://doi.org/10.3389/fendo.2018.00059.

Zhou, W., De Iuliis, G.N., Turner, A.P., Reid, A.T., Anderson, A.L., McCluskey, A., McLaughlin, E.A., and Nixon, B. (2017). Developmental expression of the dynamin family of mechanoenzymes in the mouse epididymis. Biol. Reprod. *96*, 159–173. https://doi.org/10.1095/biolreprod.116.145433.

Zhou, W., Stanger, S.J., Anderson, A.L., Bernstein, I.R., De Iuliis, G.N., McCluskey, A., McLaughlin, E.A., Dun, M.D., and Nixon, B. (2019). Mechanisms of tethering and cargo transfer during epididymosome-sperm interactions. BMC Biol. *17*, 35. 18.

STAR★METHODS

KEY RESOURCES TABLE

REAGENT or RESOURCE	SOURCE	INDENTIFIER
Antibodies		
PDIA6	Atlas Antibodies	Cat# HPA034653; RRID:AB_10601982
MSI2	Abcam	Cat# ab76148; RRID:AB_1523981
14-3-3	Abcam	Cat# ab14123; RRID:AB_300927
IDI1	Abcam	Cat# ab97448; RRID:AB_10680284
CAYBR	Sigma	Cat# SAB2107035; RRID:AB_2893393
ADCY10	Abcam	Cat# ab203204; RRID:AB_2893394
ALOX15	Abcam	Cat# ab80221; RRID:AB_1603382
RHOA	Abcam	Cat# ab86297; RRID:AB_10675086)
GAPDH	Merck	Cat# G9545; RRID:AB_796208
PT66	Merck	Cat# P5872; RRID:AB_1079609
PNA-FITC	Merck	Cat# L7381
Critical commercial assays		
Pierce™ BCA Protein Assay Kit	Thermo Fisher Scientific	Cat#23225
Endopeptidase Lys-C	Wako chemicals	Cat#129-02541
Proteomics-grade modified trypsin	Sigma	Cat#T6567
Deposited data		
Reference Proteomes – *Mus musculus*	Uniprot	UP000000589; RRID:SCR_004426
Epididymal sperm - proteomic data	This paper	PRIDE: PXD028834; RRID:SCR_003411
Mouse Genome Informatics	MGI(Smith and Eppig, 2009)	RRID:SCR_006460
The International Mouse Phenotyping Consortium	IMPC(Dickinson et al., 2016)	RRID:SCR_006158
Experimental Models: Organism /Strains		
Swiss CD1 outbred mouse strain	This paper	
Other		
RHOA Inhibitor (CT04)	Cytoskeleton.Inc.	Cat #CT04
Software and algorithms		
Proteome Discoverer 2.4	Thermo Fisher scientific	RRID:SCR_014477
Perseus	(Tyanova et al., 2016)	RRID:SCR_015753
Ingenuity Pathway Analysis	Qiagen	RRID:SCR_008653
GraphPad Prism (version 9.2.0)	Graph pad	RRID:SCR_002798
Biorender	Biorender.com	RRID:SCR_018361
Image Lab version 6.1	Bio red	RRID:SCR_014210

RESOURCE AVAILABILITY

Lead contact

Further information and requests for resources and reagents should be directed to and will be fulfilled by the Lead Contact, Brett Nixon (Brett.Nixon@newcastle.edu.au).

Materials availability

Antibodies and reagents are available from the sources listed in the key resources table. Unless otherwise specified, all reagents were purchased from Merck.

Data and code availability

- The mass spectrometry proteomics data have been deposited to the ProteomeXchange Consortium (http://proteomecentral.proteomexchange.org) via the PRIDE partner repository (Perez-Riverol et al., 2019) with the dataset identifier PXD028834 and http://dx.doi.org/10.6019/PXD028834.
- This paper does not report any original code.
- Any additional information required to reanalyze the data reported in this work paper is available from the lead contact upon request.

EXPERIMENTAL MODEL AND SUBJECT DETAILS

Ethics approval

All experimental procedures involving mice were conducted with the approval of the University of Newcastle (UoN) Animal Care and Ethics Committee (ACEC; approval number A-2018-826). Male outbred Swiss mice were obtained from a breeding colony held at the UoN central animal facility and maintained according to the recommendations prescribed by the ACEC. Mice were housed under a controlled lighting regimen (12L:12D) at 21°C–22°C and supplied with food and water *ad libitum*.

METHOD DETAILS

Isolation of epididymal spermatozoa

Immediately after adult male mice (8 week old; n = 6/biological replicate) were euthanized, their vasculature was perfused with pre-warmed Tris-buffered saline (TBS) to minimize the possibility of blood contamination. The epididymides were then removed, separated from fat and overlying connective tissue, and carefully dissected to isolate two anatomical segments of interest; the caput (proximal segment) and cauda (distal segment). The caput epididymal spermatozoa were recovered by placing the tissue in a 500 μL droplet of modified Biggers, Whitten, and Whittingham media (BWW; (Dun et al., 2012)) composed of 91.5 mM NaCl, 4.6 mM KCl, 1.7 mM $CaCl_2 \cdot 2H_2O$, 1.2 mM KH_2PO_4, 1.2 mM $MgSO_4 \cdot 7H_2O$, 25 mM $NaHCO_3$, 5.6 mM D-glucose, 0.27 mM sodium pyruvate, 44 mM sodium lactate, 5 U/ml penicillin, 5 μg/mL streptomycin, 20 mM HEPES buffer, and 3 mg/mL BSA) (pH 7.4; osmolarity 300 mOsm/kg). After multiple incisions were made with a razor blade, the spermatozoa were gently washed into the medium with mild agitation. All sperm preparations were passed through a 70 μm filter, then subjected to centrifugation (400 × g for 15 min) on a 28% Percoll/BWW density gradient. The pellet, consisting of an enriched population of caput epididymal spermatozoa (Figure S1A), was resuspended in BWW/PVA (BWW as above, with the exception that 1 mg/mL polyvinyl alcohol (PVA) was substituted in place of 3 mg/mL BSA) and re-centrifuged (400 × g for 2 min) to remove excess Percoll. Notably, BWW supplementation with BSA supports significantly higher rates of *in vitro* sperm capacitation (both in terms of the time taken to capacitate and the percentage of sperm that achieve capacitation) (Asquith et al., 2004), yet the replacement with PVA in the BWW wash buffer is designed to eliminate residual BSA prior to cell lysis and downstream applications involving protein analysis (Nixon et al., 2006). The purity and vitality of each sperm preparation was confirmed by microscopy (purity >95% spermatozoa and >70% motility; Figure S1A) consistent with previous studies (Anderson et al., 2015; Nixon et al., 2015b, 2015c).

Cauda epididymal spermatozoa were collected from the lumen via retrograde perfusion with water-saturated paraffin oil as previously described (Nixon et al., 2006). To prepare non-capacitated (NC Cauda) and capacitated (CAP Cauda) populations of cauda epididymal spermatozoa, the following media/conditions were used. Spermatozoa were held in a non-capacitated state in NC-BWW (BWW prepared as described above with the exception that 25mM NaCl was substituted in place of the 25mM $NaHCO_3$), and prepared immediately after their collection. By contrast, capacitated spermatozoa were driven to capacitate in BWW supplemented with 1 mM pentoxifylline (ptx) and 1 mM dibutyryl cyclic adenosine monophosphate (dbcAMP) and incubated at a concentration of ~10 million/mL at 37°C 5% CO_2 for 45 min (with tube lids loosened permissive of gas exchange) (Dun et al., 2012; Nixon et al., 2006). Spermatozoa were washed in BWW/PVA media after capacitation to remove any residual BSA before snap freezing and prepared for proteomic analysis as described below.

Proteomic sample preparation of spermatozoa

Samples were prepared as previously described (Humphrey et al., 2018). In brief, 250 μL of chilled lysis buffer [4% (w/v) sodium deoxycholate (SDC); 100 mM Tris-HCl (pH 8.5)], was added to each sample and immediately heated (95°C, 5 min) to inactivate endogenous proteases and phosphatases. Samples were sonicated (4 × 20 s cycles, 75% output power), and an aliquot taken to determine protein concentration using a bicinchoninic acid assay (BCA). All samples were diluted to equal protein amounts (120 μg) in 270 μL of lysis buffer in 2 mL deep well plates. Samples were reduced and alkylated [100 mM Tris(2-carboxyethyl)phosphine hydrochloride; 400 mM 2-chloroacetemide], using a Thermomixer (Eppendorf; Hamburg, Germany) in which samples were incubated for 5 min at 45°C (1,500 rpm). Enzymatic digestion was achieved using Lys-C and trypsin, at an enzyme-to-substrate ratio of 1:100 (w/w) and incubated overnight at 37°C with shaking (1,500 rpm). Fifty μL peptides were aliquoted into fresh PCR tubes for each sample, comprising ~7.5 μg. Each sample was diluted 1:1 with HPLC grade water to lower SDC concentration below 1% and vortexed briefly, followed by the addition of 100 μL of 99% ethylacetate/1% TFA and mixing for 5 min at room temperature (2,000 rpm). The resultant

200 μL was transferred to styrenedivinylbenzene-reverse phase sulfonated (SDB-RPS) StageTips (Rappsilber et al., 2007) for desalting. StageTips were centrifuged at 1,500 × g for 3 min and subsequently washed with 100μL 99% ethylacetate/1% TFA (1,500 × g, 3 min). Finally, StageTips were washed with 100 μL each of 99% isopropanol/1% TFA and 0.2% TFA/5% acetonitrile, eluted with 60 μL of 5% NH_4OH/80% acetonitrile, dried by vacuum concentration and re-suspended in MS loading buffer (2% acetonitrile/0.3% TFA). Purified sperm peptides were subjected to offline high pH fractionation, prior to analysis by high resolution nano liquid chromatography-tandem mass spectrometry (nLC-MS/MS).

nLC-MS/MS analysis

Reverse phase nLC-MS/MS was performed on 12 high pH concatenated fractions using an Orbitrap Exploris 480 MS coupled to a Dionex Ultimate 3000RSLC nanoflow high-performance liquid chromatography system (Thermo Fisher Scientific, Waltham, MA). Samples were loaded onto an Acclaim PepMap 100 C18 75 μm × 20 mm trap column (Thermo Fisher Scientific) for pre-concentration and online de-salting. Separation was then achieved using an EASY-Spray PepMap C18 75 μm × 250 mm column (Thermo Fisher Scientific), employing a curved gradient of acetonitrile (2–35%, 46 min; 35–95%, 4 min; 95%–2%, 10 min) over 60 min. Full MS/data dependent acquisition MS/MS mode was utilized on Xcalibur (Thermo Fisher Scientific; version 4.2.47) with the Orbitrap mass analyzer set at a resolution of 60,000, to acquire full MS with an m/z range of 350–1500, incorporating a normalized automatic gain control target of 300% and maximum fill times of 50 ms. The 20 most intense multiply charged precursors were selected for higher-energy collision dissociation fragmentation with a collisional energy of 30%. MS/MS fragments were measured at an Orbitrap resolution of 15,000 using standard mode for automatic gain control target and maximum fill times of 120 ms.

Immunofluorescence

Spermatozoa were fixed in 4% PFA, washed in 50 mM glycine/phosphate-buffered saline (PBS), and settled onto poly-L-lysine-treated coverslips at 4°C overnight. All subsequent incubations were performed in a humidified chamber, and all antibody dilutions and washes were conducted in PBS. Fixed cells were permeabilized in 0.2% Triton X-100/PBS for 10 min and blocked in 3% (w/v) BSA in PBS for 1 h at 37°C. Slides were then sequentially labeled with primary antibodies (diluted between 1:50 to 1:250) overnight at 4°C. After incubation, the slides were washed three times, then incubated in appropriate Alexa Fluor 488 conjugated secondary antibodies (diluted 1:400) for 1 h at 37°C. Cells were then washed and mounted in antifade reagent (Mowiol 4–88). Labeled cells were viewed on an Axio Imager A2 microscope (Carl Zeiss MicroImaging, Inc., Jena, Germany) equipped with epifluorescent optics and images captured with Zeiss Axiocam 305 mono camera.

SDS-PAGE and immunoblotting

For the purpose of orthogonal validation, sperm proteins were extracted from samples independent of those used for mass spectrometry using a modified SDS-PAGE sample buffer (2% w/v SDS, 10% w/v sucrose in 0.1875 M Tris, pH 6.8) supplemented with protease inhibitor cocktail (Roche, Basel, Switzerland). Samples were boiled at 100°C for 5 min after which insoluble matter was pelleted by centrifugation at 20,000 × g for 10 min and the quantity of soluble protein remaining in the supernatant was estimated using a DC Protein Assay in accordance with the manufacturer's instructions (Bio-Rad Laboratories, Hercules, CA). Similarly, proteins were also extracted using different methods such as RIPA and SDC buffers. For RIPA buffer (150 mM NaCl, 1% v/v Triton X-100, 0.5% w/v sodium deoxycholate, 0.1% w/v SDS, 50 mM Tris pH 8) the protein was shaken at 4°C for 20 min, and for SDC (4% w/v SDC and 100 mM Tris-HCl pH8.5), protein was sonicated 4 × 10 s. Both cell lysate suspensions were then centrifuged, and protein quantified as above. Extracted proteins were boiled for 5 min in SDS-PAGE sample buffer (2% v/v mercaptoethanol, 2% w/v SDS, and 10% w/v sucrose in 0.1875 M Tris, pH 6.8, with bromophenol blue) prior to being resolved by SDS-PAGE and transferred onto nitrocellulose membranes. Membranes were blocked with 3% w/v BSA in TBS and 0.1% v/v polyoxyethylenesorbitan monolaurate (Tween 20; TBS-T; pH 7.4) for 1 h before being probed with 1 μg/mL concentration of appropriate primary antibodies diluted in TBS-T containing 1% w/v BSA overnight at 4°C. Blots were washed three times in TBS-T followed by incubation with an appropriate horseradish peroxidase (HRP)-conjugated secondary antibodies diluted 1:2500 in 1% w/v BSA/TBS-T for 1 h at room temperature. Following three washes in TBS-T, labeled proteins were detected using an enhanced chemiluminescence kit (GE Healthcare, Chicago, IL) and visualized on a ChemiDoc MP (Bio-Rad, Hercules, California, USA) (Skerrett-Byrne et al., 2021c; Zhou et al., 2017). For the validation of each candidate protein, three immunoblots were performed using three independent biological samples, with each blot being subjected to stripping and re-probing with the loading control α-GAPDH antibody in preparation for densitometric analyses of relative band labeling intensity.

RHOA inhibition studies

Initial cytotoxicity testing was undertaken whereby cauda epididymal spermatozoa were dispersed into NC-BWW and separated into four equal populations prior to the addition of the RHOA inhibitor at concentrations of either 0.5, 1 or 2 μg/mL (CT04; Cytoskeleton Inc., Colorado, USA) or an equal volume of BWW medium (control). The spermatozoa were pre-incubated with or without CT04 for 0, 60 and 120 min at 37°C, before sperm viability was assessed (Figure S6A). Following this, cauda epididymal spermatozoa were dispersed into NC-BWW and separated into two equal populations prior to the addition of the RHOA inhibitor (1 μg/mL) to the treatment group and an equal volume of medium to the control group. Spermatozoa were pre-incubated with or without CT04 for 1 h at 37°C, before being driven to capacitate (as described above) for a further 45 min at 37°C in an atmosphere of 5% CO_2. At the end of

each incubation, the sperm populations were assessed for motility and were then either fixed in 4% paraformaldehyde (for assessment of spontaneous acrosome reaction rates) or induced to undergo an acrosome reaction with the calcium ionophore, A23187 (Merck) (induced). For the latter treatment, A23187 was added at a final concentration of 2.5 μM, alongside a DMSO vehicle control, and incubated 37°C for 30 min. After induction of acrosomal exocytosis, spermatozoa were incubated in hypoosmotic swelling medium for 1 h at 37°C and then fixed in 4% paraformaldehyde (Figure S6B). Spermatozoa were then washed in 50 mM glycine/PBS and air dried onto 12-well slides in preparation for labeling with the acrosome marker, PNA-FITC (lectin from *Arachis hypogea* [peanut]) (Merck). Spermatozoa were first permeabilized with ice-cold methanol for 10 min followed by incubation in PNA-FITC (5 μg/mL) for 20 min at 37°C, and 3 final washes in PBS. Spermatozoa were examined using a Zeiss Axio Imager 2 and the percentage of acrosome reacted cells (i.e. those without florescent labeling of their acrosome) was calculated (Cafe et al., 2020).

QUANTIFICATION AND STATISTICAL ANALYSIS

Proteomic data processing and analysis

Consistent with previous studies (Skerrett-Byrne et al., 2021a, 2021b, 2021c), database searching of each sample group's raw files were performed separately using Proteome Discoverer 2.4 (Thermo Fisher Scientific). SEQUEST HT was used to search against the UniProt *Mus musculus* database (25,285 sequences, downloaded 30th July 2020). Database searching parameters included up to two missed cleavages, a precursor mass tolerance set to 10 ppm and fragment mass tolerance of 0.02 Da. Trypsin was designated as the digestion enzyme. Cysteine carbamidomethylation was set as a fixed modification while acetylation (K, N-terminus) and oxidation (M) were designated as dynamic modifications. Interrogation of the corresponding reversed database was also performed to evaluate the false discovery rate (FDR) of peptide identification using Percolator on the basis of q-values, which were estimated from the target-decoy search approach. To filter out target peptide spectrum matches over the decoy-peptide spectrum matches, a fixed FDR of 1% was set at the peptide level. Each protein list was exported from Proteome Discoverer 2.4 as a Microsoft Excel file and further refined to include only those with a quantitative value (label-free quantification; Minora Feature Detector) in each of the three biological replicates and two or more unique peptides (Degryse et al., 2018; Murray et al., 2020; Nixon et al., 2019b, 2019c; Skerrett-Byrne et al., 2021b, 2021c). By exception, proteins with one unique matched peptide were included in the analysis if the coverage sequence (%) of that protein was equal to or greater than the average sequence coverage of the full complement of proteins with two or more unique peptides. All sample groups were combined, and raw abundance values were normalized using Perseus, version 1.6.10.43 (Tyanova et al., 2016), in addition to the generation of scatterplots, principal component analysis, volcano plots and heatmaps. Basic data handling, if not otherwise stated, was conducted using Microsoft Excel 2016 (Version 16.0.4966.1000, Microsoft Corporation, Redmond, WA) and GraphPad Prism version 8.4.3 for Windows (GraphPad Software; San Diego, CA).

Ingenuity pathway analysis and phenotype comparison

Core proteomic inventories of each sample group containing UniProt accession were analyzed using Ingenuity Pathway Analysis software (IPA; Qiagen, Hilden, Germany) as previously described (Degryse et al., 2018; Skerrett-Byrne et al., 2021a, 2021b, 2021c; Smyth et al., 2022). Proteomic datasets (6,235/6,381; 98%) were analyzed on the basis of predicted subcellular location and classification (other excluded), in addition to 'molecular and cellular functions' and 'physiological system development and function' using the IPA p value enrichment score (Kramer et al., 2014). To elucidate the most significant changes in our analyses, we applied a stringency criterion of -$\log_{10}$ p value of $\geq$1.3 for each group. For comparative analyses, UniProt accession numbers and transformed ratios were analyzed. Canonical pathways, upstream regulators, and disease and function analyses were assessed using p value and *Z* score; the latter being a prediction scoring system of protein/pathway activation or inhibition based upon statistically significant patterns in the dataset in combination with prior biological knowledge manually curated in the Ingenuity Knowledge Base. We applied strict cut-offs of -$\log_{10}$ p value of $\geq$1.3 and a *Z* score of ±2 (Skerrett-Byrne et al., 2021b, 2021c). For disease and function assessment the analysis was restricted to 'molecular and cellular functions' and 'physiological system development and function'. The core proteomic inventory of epididymal spermatozoa was also compared against the full complement of Mouse Genome Informatics (MGI) (Smith and Eppig, 2009) and The International Mouse Phenotyping Consortium (IMPC) (Dickinson et al., 2016) datasets to identify proteins with known phenotypes associated with impaired sperm functions/processes, morphological abnormalities or male fertility disorders. Each epididymal spermatozoa proteome was mapped on UniProt to extract UniProt and EMBL-EBI GO specific sperm cell domain annotations.

Immunoblot densitometry

Image Lab software (Bio-Rad) was used to perform densitometric analysis of all immunoblots. Briefly, each lane was labeled and the correct sized band of the protein of interest was marked. The 'lane profile' tool was used to define the correct lane and band size widths and to confirm uniformity. An 'analysis table' was then generated to contain the densitometric volume for each band in each lane (adjusted by subtraction of background). This process was replicated with the corresponding α-GAPDH immunoblot image to enable the volume of the band of interest to normalized against that of the comparable α-GAPDH loading control band volume for each lane. The fold change of band volume from cauda epididymal sperm samples was calculated relative to that of the caput epididymal sperm samples, thereby enabling determination of changes in the relative abundance of each protein of interest. Three such analyses were conducted on independent biological samples for each protein of interest.

STATISTICAL ANALYSIS

Proteomic analyses were performed using sperm cell populations collected from two anatomical segments of interest; the caput (proximal region) and cauda (distal region) with a portion of cauda epididymal spermatozoa induced to undergo capacitation *in vitro* as described above (n = 3 biological replicates collected from 6 individual mice/biological replicate). Differentially accumulated sperm proteins were defined as those with a fold-change ± 2 and p value $\leq$ 0.05. All other data were assessed for normality using a Shapiro-Wilk normality test. Normally distributed data were analyzed by unpaired Student's t-tests to detect differences between treatment groups. Data not normally distributed were analyzed by a Mann-Whitney test. Differences between groups were considered significant when p $\leq$ 0.05. The number of biological replicates used in each experiment are presented in figure captions. Graphical data were prepared using GraphPad Prism (version 9.2.0) and are presented as mean values ±SEM.